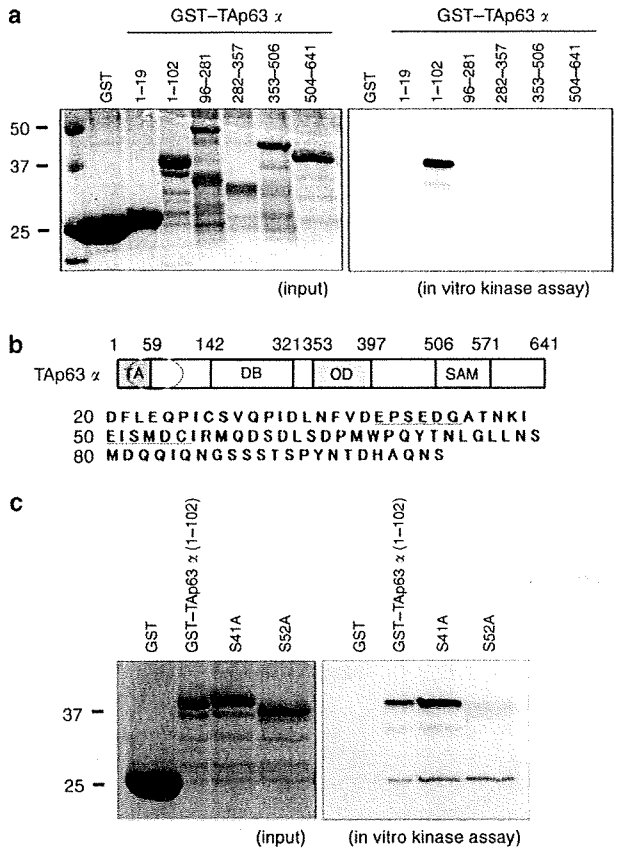

Figure 3 Plk1 directly phosphorylates Ser-52 of TAp63. (**a**) *in vitro* kinase assay. GST and GST-tagged TAp63alpha deletion mutants were incubated with the active form of Plk1 in the presence of [γ-^{32}P]ATP. The reaction mixtures were separated by SDS–PAGE (polyacrylamide gel electrophoresis) and subjected to autoradiography. (**b**) A sequence (D/E)*X*(S/T)ΦD/E) (where *X* is any amino acid and Φ is hydrophobic amino acid) was identified as a consensus motif for Plk1-dependent phosphorylation. According to the search for a putative phosphorylation site(s) targeted by Plk1 within the amino acid sequence of TAp63 (residues 20–96), related motifs, (39EPSEDG44 and 50EISMDC55), were in the NH2-terminal portion of TAp63alpha. (**c**) *in vitro* kinase assay. GST and GST-TA63alpha-(1–102)S41A, and GST-TA63alpha-(1–102)S52A were incubated with the active form of Plk1 in the presence of [γ-^{32}P]ATP. The reaction mixtures were separated by SDS–PAGE and subjected to autoradiography.

however, these phenomena were attenuated by co-transfection of Plk1, and KD Plk1 failed to attenuate it (Figure 5a). To study the molecular mechanism of the effect of Plk1-induced phosphorylation on the function of TAp63, we checked the protein stability of TAp63alpha in the presence of Plk1 or KD Plk1(K82M). As shown in Figures 5b and c, Plk1 clearly decreased the protein stability of TAp63alpha. On the other hand, KD Plk1(K82M) did not modify the protein stability of TAp63alpha. In addition, the Plk1-related degradation of TAp63 was not attenuated by a proteasome inhibitor MG132 (data not shown), consistent with the phenomenon in TAp73/Plk1 experiments (Koida *et al.*, 2008). These results suggest that Plk1 downregulates the protein stability of TAp63 by its phosphorylation through a proteasome-independent pathway and suppresses TAp63-induced cell death.

Expression of Plk1 and p63 in liver tumor cells

Earlier our laboratory reported that Plk1 is highly expressed in hepatoblastoma samples and that patients with a high expression of Plk1 showed significantly poorer prognosis than those with a low expression (Yamada *et al.*, 2004), indicating Plk1 involvement in carcinogenesis and its potential as a therapeutic target in liver cell malignancy. As the above results indicate the significance of Plk1/TAp63 in the regulation of cell death of cancer cells, we studied the expression level of Plk1 and p63 in liver tumor cell lines (Figure 6a). We used one hepatoblastoma cell line (Huh6) and five HCC cell lines. From the results of reverse transcription (RT)–PCR and western blotting, a considerable expression of Plk1 was observed in liver tumor cell lines. Also, TAp63 was expressed in all liver tumor cell lines and the deltaNp63 expression was observed in HLF and PLC/PRF/5 cells.

Significance of TAp63 in Plk1 knockdown-induced apoptosis of liver tumor cells

Next, we carried out a knockdown experiment of Plk1 using siRNA in liver tumor cells (Huh6, HLE and HLF cells). FACS analysis suggested that Plk1 knockdown induced an increase in the sub-G0/G1 fraction not only in p53 wild-type Huh6 cells but also in p53 mutant-type HLE cells (Figure 6b). As p53 is mutated in HLE cells, this suggested the significance of TAp63 and/or p73 in Plk1 knockdown-induced apoptosis of liver tumor cells; however, the sub-G0/G1 fraction did not increase in HLF cells. In both HLE and HLF cells, p53 was mutated, and TAp63 and p73 were considerably expressed, although the expression of deltaNp63 was detected only in HLF cells (Figure 6a and Supplementary data), suggesting the possible anti-apoptotic effect of deltaNp63 in Plk1 knockdown-induced apoptosis. Next, we studied the influence of Plk1 knockdown on p53 family downstream effectors in liver tumor cells by RT–PCR experiments (Figure 6c). Plk1 knockdown transactivated the p53 family downstream effectors $p21^{Cip1/WAF1}$, *GADD45* and *PUMA* in Huh6 cells, and $p21^{Cip1/WAF1}$, *14-3-3σ* and *PUMA* in HLE cells.

As a result of Plk1 single knockdown, we found significant TAp63 in Plk1 knockdown-induced apoptosis pathways. Next, we carried out double knockdown experiments of Plk1/TAp63 using HLE cells. Plk1 single knockdown increased cell death, but this was suppressed by double knockdown of Plk1/TAp63 (Figure 6d). Furthermore, we examined the influence of double knockdown of Plk1/TAp63 on the expression of p53 family downstream effectors by RT–PCR (Figure 6e). *PUMA*, *14-3-3σ* and $p21^{Cip1/WAF1}$ expression levels were increased by Plk1 single knockdown, and double knockdown of Plk1 and TAp63 successfully abolished the increase in p53 family downstream effectors by the single knockdown.

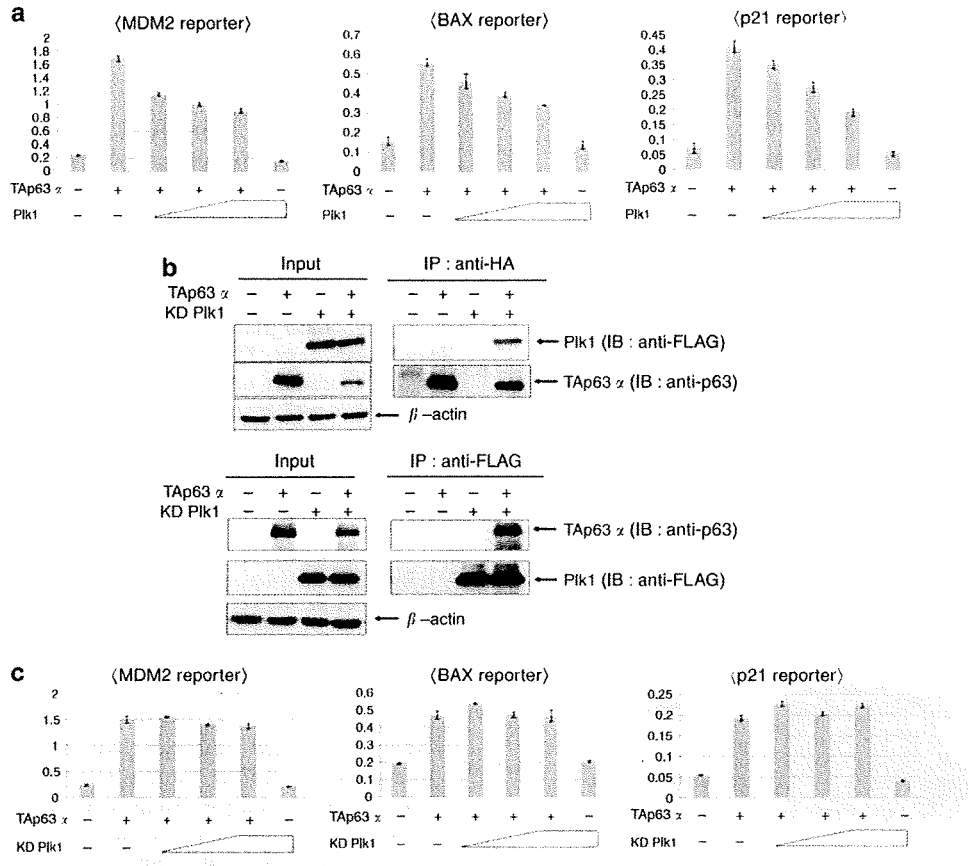

Figure 4 Plk1 represses TAp63-mediated transcriptional activation. (**a** and **c**) H1299 cells (5×10^4 cells) were co-transfected with a constant amount of TAp63alpha expression plasmid (25 ng), 100 ng of p53/p63-responsive luciferase reporter construct bearing *p21*$^{Cip1/WAF1}$, *BAX* or *MDM2* promoter and 10 ng of *Renilla* luciferase reporter plasmid (pRL-TK) in the presence or absence of increasing amounts of FLAG-Plk1 expression plasmid (**a**) or FLAG-Plk1(K82M) expression plasmid (**c**) (50, 100 and 200 ng). To standardize the amounts of plasmid DNA per transfection, pcDNA3 was added to yield 510 ng of plasmids. At 48 h after transfection, cells were lysed, and their luciferase activities were measured. Data were normalized and presented as mean values ± s.d. of three independent experiments. (**b**) Plk1(K82M) retains the ability to interact with TAp63 in cells. COS-7 cells were transiently transfected with FLAG-KD Plk1 and/or HA-TAp63 expression plasmids, immunoprecipitated with monoclonal anti-HA antibody (clone 3F10, Roche) and monoclonal anti-FLAG antibody (clone M2, Sigma), and immunoblotted with monoclonal anti-FLAG antibody and monoclonal anti-p63 antibody (clone 4a4) as indicated, to observe the interaction.

Possible role of Plk1/p63 in cancer stem cell fraction of liver tumor cells

Previous research showed that the involvement of Plk1 is crucial for the metaphase–anaphase transition. Plk1 mRNA and protein levels are coordinately regulated during cell-cycle progression and are highest in the mitotic phase (Winkles and Alberts, 2005; Eckerdt and Strebhardt, 2006). These observations suggested that Plk1 expression may be modest in the cancer stem cell fraction and that have a less significant role in cell death as cancer stem cells are generally accumulated in the Go/G1 phase (Zhou and Zhang, 2008). To examine expression levels of Plk1 and p63 in the cancer stem cell fraction, we carried out real-time PCR using the side population (SP) fraction and non-SP fraction of liver tumor cells. Surprisingly, the result suggested that both Plk1/p63 are highly expressed in the SP fraction compared with in the non-SP fraction (Figure 7a). Furthermore, the expression level of TAp63 was higher than that of deltaNp63 in the SP fraction of Huh7 cells, and almost equal to PLC/PRF/5 cells (Figure 7b). An analysis of the p63 downstream molecules in the SP and non-SP fraction indicated that p63 activities were repressed in the SP fraction except for the p21 activation in PLC/PRF/5 cells (Figure 7c), suggesting the possibility that p21 might be induced in a p53/TAp63-independent manner. These results suggest the considerable role of Plk1/p63 in the development of cancer stem cell-targeted therapy for liver tumor cells.

Discussion

Post-translational modification of p53 family members is a key phenomenon in their regulation (Shieh *et al.*, 1997); however, the regulation of p63 through post-translational modification has been studied only recently (Huang *et al.*, 2004; Ghioni *et al.*, 2005). From these studies, it has been suggested that p63 protein levels can change rapidly as a result of post-translational mod-

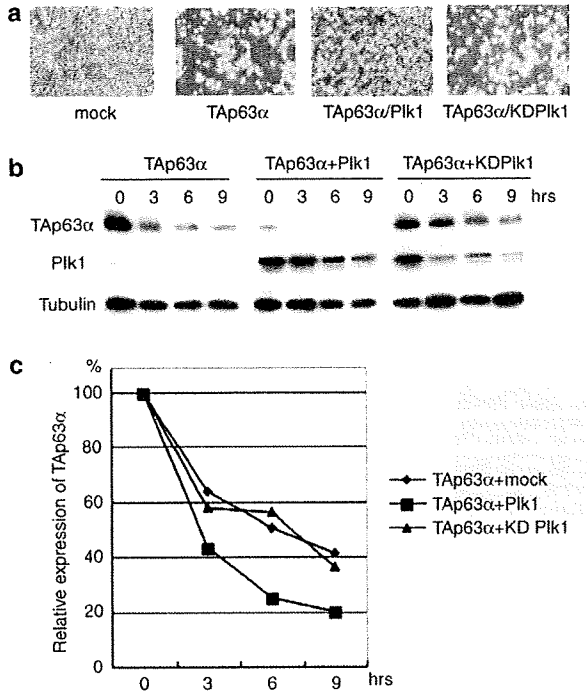

Figure 5 Plk1 downregulates the protein stability of TAp63 by its phosphorylation and suppresses TAp63-induced cell death. (**a**) H1299 cells were transfected with TAp63alpha alone or together with Plk1 or KD Plk1. At 24-h post-transfection, the cells were observed. (**b**) Decreased half-life of TAp63alpha in the presence of Plk1. Hep3B cells were transfected with TAp63lpha alone or together with Plk1 or KD Plk1. At 24-h post-transfection, the cells were treated with cycloheximide (50 μg/ml) and harvested at the indicated time points after the addition of cycloheximide. Cell lysates were analysed by SDS–PAGE (polyacrylamide gel electrophoresis) and immunoblotting. (c) Densitometric analysis of all TAp63alpha protein bands relative to tubulin was measured using NIH ImageJ software and plotted on a graph. The value of 0-h signals was indicated as 100%.

ification. At present, limited studies of the phosphorylation status of p63 have been reported (Westfall *et al.*, 2005; Suh *et al.*, 2006). DNA damage induces both the phosphorylation of p63 and its binding to p53 cognate DNA sites, and these events are linked to oocyte death (Suh *et al.*, 2006). TAp63 is constitutively expressed in female germ cells during meiotic arrest and is essential in the process of DNA-damage-induced oocyte death not involving p53. Furthermore, the phosphorylation of TAp63γ, but not deltaNp63γ, by IκB kinase β (IKKβ) was reported, although the exact amino acid residue for phosphorylation was not determined (MacPartlin *et al.*, 2008). The IKKβ-related phosphorylation of TAp63γ was also induced by γ-radiation. Upon ultraviolet radiation, deltaNp63α was phosphorylated at the ser-66/68 (in TAp63α, Ser-160/162) residues and led to ubiquitin-mediated degradation, suggesting that the protein stability of deltaNp63 is controlled by phosphorylation of different amino acid residues compared with that of TAp63 (Westfall *et al.*, 2005).

In this study, we reported that Plk1 directly interacts with p63 and the Ser-52 residue of TAp63 is phosphorylated by Plk1 (Figure 3). This Plk1-induced TAp63 phosphorylation might not to be related to the DNA-damage-induced phosphorylation of TAp63, as Plk1 was shown to be downregulated in response to DNA damage (Smits *et al.*, 2000; van Vugt *et al.*, 2001); however, the Ser-52 phosphorylation of TAp63 after DNA damage should be examined for the following reasons: (1) IKKβ-induced phosphorylation of TAp63 was shown in the TA domain of TAp63γ and was related to TAp63γ stabilization in response to γ-radiation (MacPartlin *et al.*, 2008) and (2) radiation-induced phosphorylation/activation of p63 in oocytes occurs in TAp63 but not in deltaNp63 (Suh *et al.*, 2006). Interestingly, the previously reported p63 phosphorylation was related to protein stabilization, upregulation of activity and induction of apoptotic cell death (Westfall *et al.*, 2005; Suh *et al.*, 2006). This study, however, clarified that phosphorylation by Plk1 results in protein degradation and suppression of the transcriptional activity of TAp63alpha (Figure 5b), consistent with the inactivation of transcriptional activity in p53 (Ando *et al.*, 2004) and p73alpha (Koida *et al.*, 2008). It can be noted that, this Plk1-related TAp63 degradation was affected by cell density of Hep3B cells (data not shown), suggesting that further analysis of p63 phosphorylation and its effect on degradation will be required in future.

The study of Ser-52 phosphorylation not only in DNA damage response but also in oncogene-related stimulation will contribute to understanding the exact role of Plk1-related tumorigenesis in many malignancies. Anti-phosphor-Ser-52 TAp63 antibody will be an indispensable tool for those studies and phosphorylation of Ser-52 among TAp63 isoforms, TAp63α/TAp63β/TAp63γ, should be addressed in various malignancies. Another interesting finding in our study is that both Plk1/p63 were highly expressed in the SP fraction of liver tumor cells compared with the non-SP fraction, although p63 downstream molecules were not induced in SP fraction except for p21 (Figure 7), suggesting that Plk1 has an important function in preventing apoptotic cell death in tumorigenesis through the inactivation of p53 family members in tumor-initiating cells; therefore, the functional interaction of this Plk1–p53 family protein appears to be a candidate for tumor-initiating cell-targeted therapy.

Despite strong and continuing emphasis on the involvement of the p53 family in tumorigenesis because of the tumor suppressive role of the founding member p53, it now seems evident that the remaining family members, p63 and p73, are highly involved in regulating the development of different tissues (Candi *et al.*, 2007). In particular, lines of evidence indicate that the main role of p63 lies in the regulation of epithelial development and, in particular, in the formation of the epidermis (Mills *et al.*, 1999; Yang *et al.*, 1999); however, the exact molecular regulation mechanism of TAp63/deltaNp63 transcriptional activities related to development and tumor suppression remains to be elucidated. Recently, several target genes of TAp63 in epithelial development have been identified, for example, IKKa/GATA-3 (Candi *et al.*, 2006), Jagged-1&-2 (Sasaki *et al.*,

2002), Hes-1/Hey-1&-2 (Nguyen *et al.*, 2006), K14 (Koster *et al.*, 2004) and p21 (Westfall *et al.*, 2003). We also reported that TAp63-dependent induction of growth differentiation factor 15 (GDF15) has a critical function in the regulation of keratinocyte differentiation (Ichikawa *et al.*, 2008). Investigation of the role of the Ser-52 phosphorylation of TAp63 in selective transactivation of these specific target genes will be an interesting research project to understand development regulation.

Furthermore, it was recently reported that Plk1 homozygous null mice were embryonic lethal and early Plk1−/− embryos failed to survive after the eight-cell stage. Immunocytochemistry studies showed that Plk1 null embryos were arrested outside the mitotic phase (Lu *et al.*, 2008). These observations suggest that the Plk1/p63 relationship may play an important role not only in later epithelial tissue organization but also in early embryonic development.

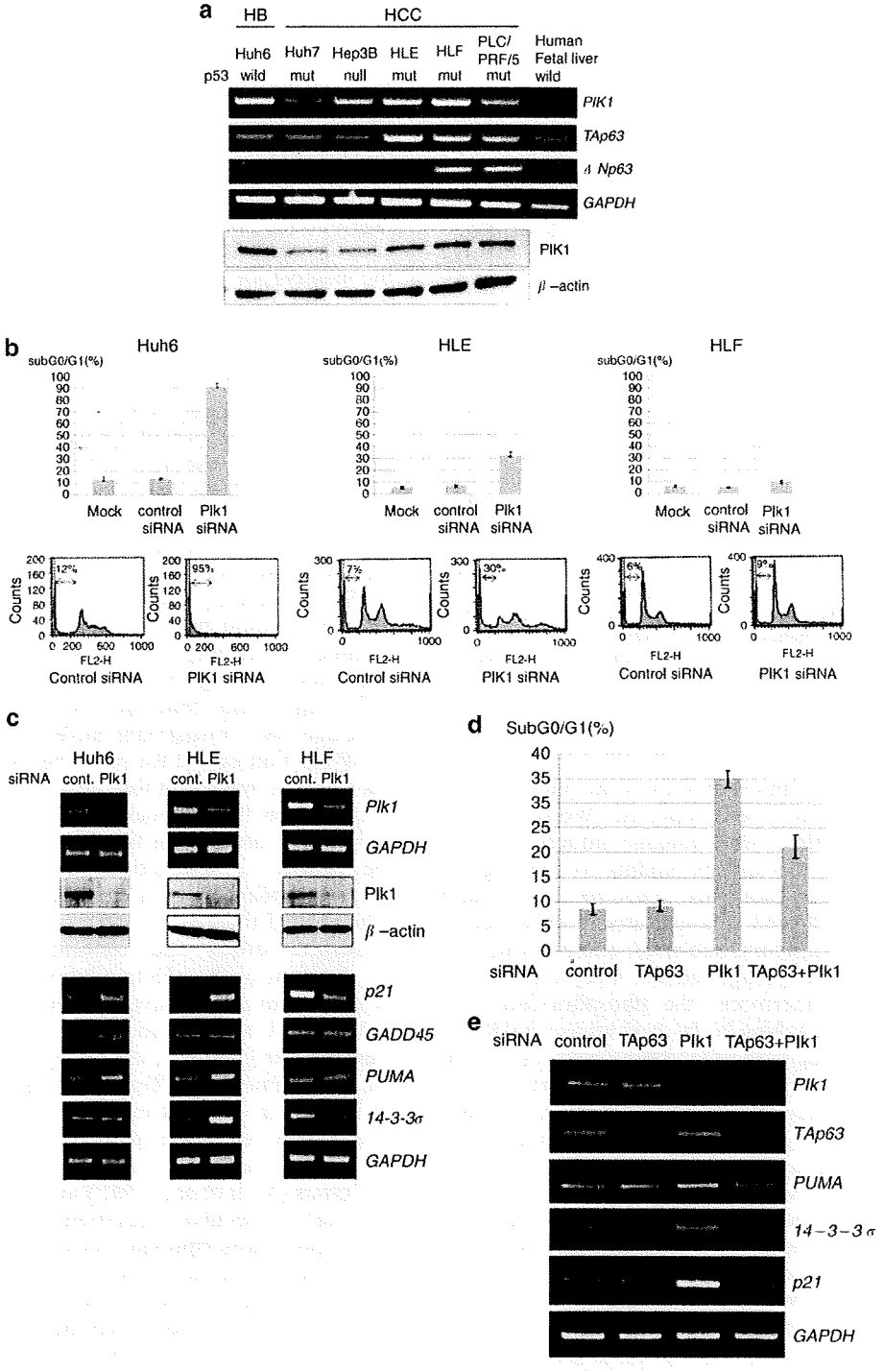

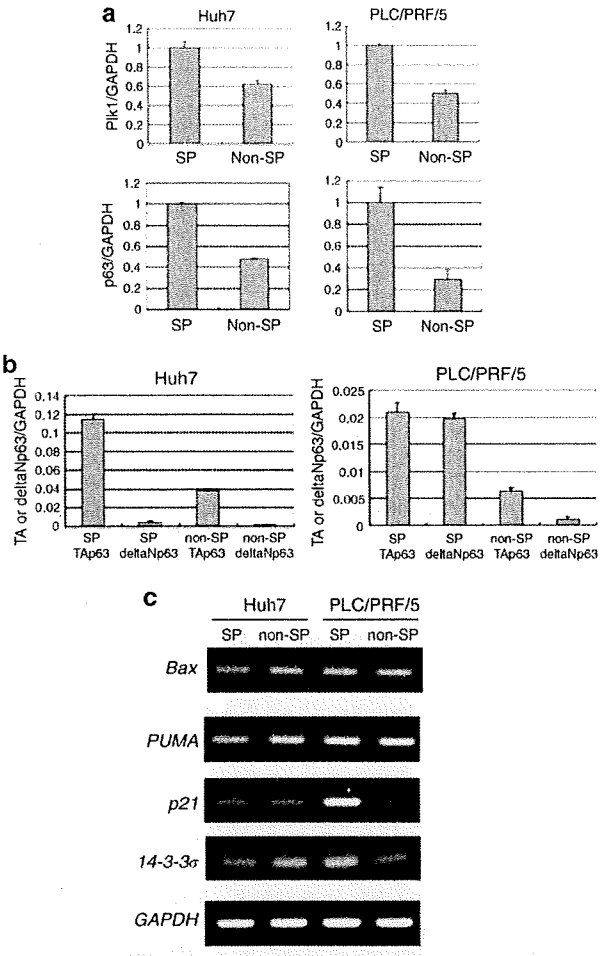

Figure 7 Possible role of Plk1/p63 in tumor-initiating cell fraction of liver tumor cells. (**a**) Using the side population (SP) fraction and non-SP fraction of liver tumor cells, expression levels of Plk1 and p63 were examined by real-time PCR analysis. Data were normalized and presented as the mean values ± s.d. of three independent experiments. (**b**) TAp63 and deltaNp63 expression levels in the SP fraction of liver tumor cells. Expression levels of TAp63 and deltaNp63 were examined by real-time PCR analysis. Data were normalized and presented as the mean ± s.d. of three independent experiments. (**c**) Semiquantitative reverse transcription (RT)–PCR analysis of the expression of *Bax*, *Puma*, *14-3-3σ* and *p21* in SP and non-SP cells.

Materials and methods

Cell culture

The African green monkey kidney cell line COS-7, human lung carcinoma cell line H1299, human hepatoblastoma cell line Huh6, HCC cell lines Huh7, Hep3B, HLE, HLF and PLC/PRF/5, and keratinocyte-like HaCaT cells were maintained in Dulbecco's modified Eagle's medium supplemented with 10% heat-inactivated fetal bovine serum (Invitrogen, Carlsbad, CA, USA), 50 μg/ml of penicillin and streptomycin each (Invitrogen). These cells were incubated at 37 °C in an atmosphere containing 5% CO_2.

RNA extraction and RT–PCR

Total RNA extraction, cDNA synthesis and semi-quantitative RT–PCR were carried out as described earlier (Koida *et al.*, 2008). The specific primers were indicated as supplements (Supplementary data). The expression of GAPDH (glyceraldehyde-3-phosphate dehydrogenase) was measured as an internal control.

SP analysis

Side population analyses were conducted as described earlier (Chiba *et al.*, 2006). We have studied the hepatocellular markers such as AFP (alpha-fetoprotein) or cytokeratin19 (CK19) of SP and non-SP cells that are obtained by sorting, and a large number of cells positive for both markers were observed in SP cells (Chiba *et al.*, 2006).

Quantitative real-time RT–PCR of Plk1 and TAp63

Polymerase chain reaction of TAp63 was carried out using TaqMan technology (Applied Biosystems, Foster City, CA, USA). Gene expression assay primer and probe mixes were used for TAp63 and GAPDH (assay IDs: Hs00186613_m1 and 4310884E, respectively), and reactions were carried out according to the manufacturer's protocol. Polymerase chain reaction of Plk1 was carried out using SYBR Green technology (Takara Bio, Otsu, Shiga, Japan). PCR was carried out using an ABI Prism 7700 Sequence Detection System (Perkin-Elmer/Applied Biosystems, Carlsbad, CA, USA). Primers were indicated in Supplementary data.

Protein extraction and western blot analysis

Extraction of cellular proteins, protein concentration analysis, SDS–PAGE, protein transfer and western blot analysis were carried out as described in Supplementary data.

Figure 6 Plk1 knockdown transactivates p53 family downstream effectors and induces apoptotic cell death. (**a**) Semiquantitative reverse transcription (RT)–PCR and western blotting of Plk1 and p53 family in hepatoblastoma and hepatocellular carcinoma cell lines. (**b**) FACS analysis of liver tumor cells subjected to small interfering RNA (siRNA)-mediated knockdown of endogenous Plk1. Cells were transfected with 10 nM of control siRNA or Plk1 siRNA. At 48 h after transfection, both floating and attached cells were collected by low-speed centrifugation. The cells were then stained with propidium iodide (50 μg/ml) in the presence of 50 μg/ml of RNase A for 30 min at room temperature. The DNA content indicated by propidium iodide staining was analysed using a FACSCalibur flow cytometer. (**c**) RT–PCR analysis of siRNA-mediated knockdown of endogenous Plk1 in liver tumor cells. Cells were transfected with 10 nM of control siRNA or Plk1 siRNA. At 48 h after transfection, total RNA was prepared and analysed for expression levels of $p21^{Cip1/WAF1}$, *GADD45*, *PUMA* and *14-3-3σ*. Amplification of *GAPDH* serves as an internal control. (**d**) FACS analysis of siRNA-treated cells. HLE cells were transfected with TAp63 siRNA and/or Plk1 siRNA. To standardize the amounts of siRNA per transfection, control siRNA was added to yield 15 nM of siRNA. At 48 h after transfection, both floating and attached cells were collected by low-speed centrifugation. Cells were then stained with propidium iodide (50 μg/ml) in the presence of 50 μg/ml of RNase A for 30 min at room temperature. The DNA content indicated by propidium iodide staining was analysed using a FACSCalibur flow cytometer. (**e**) RT–PCR analysis of siRNA-treated cells. HLE cells were transfected with TAp63 siRNA and/or Plk1 siRNA. To standardize the amounts of siRNA per transfection, control siRNA was added to yield 15 nM of siRNA. At 48 h after transfection, total RNA was prepared and analysed for expression levels of $p21^{Cip1/WAF1}$, *PUMA* and *14-3-3σ*. Amplification of *GAPDH* serves as an internal control.

Immunoprecipitation and western blot analysis
For the immunoprecipitation of Plk1 and p63, COS-7 cells were transiently transfected with 2 μg of the expression plasmids for FLAG-Plk1 and or HA-TAp63alpha using Lipofectamine 2000 Transfection Reagent (Invitrogen). Protein extraction was carried out as described earlier. The extracts were incubated with the monoclonal anti-FLAG (clone M2, Sigma, St Louis, MO, USA) or monoclonal anti-HA antibody (clone 3F10, Boehringer Roche, Mannheim, Germany) at 4 °C for 8 h. Immunocomplexes were precipitated with protein G-Sepharose beads at 4 °C for 30 min, which were then pelleted by centrifugation at 15 000 *g* for 5 min. The precipitates were washed with lysis buffer three times at 4 °C, resuspended in 30 μl of SDS sample buffer and treated at 100 °C for 5 min. Proteins were then resolved by 8% SDS–PAGE, and transferred onto Immobilon-P membranes (Millipore, Bedford, MA, USA). The protein complex was detected by western blot analysis using monoclonal anti-FLAG or monoclonal anti-p63 antibodies.

GST pull-down assay
cDNA fragments encoding the indicated deletion mutants of TAp63alpha were generated by a PCR-based strategy, and subcloned into GST fusion protein expression plasmid pGEX-4T-1 (GE Healthcare, Piscataway, NJ, USA). GST and GST–TAp63alpha fusion proteins were expressed and purified using glutathione-Sepharose beads (Amersham Biosciences). FLAG-Plk1 was radiolabeled *in vitro* using the TNT Quick Coupled transcription/translation system (Promega, Madison, WI, USA) in the presence of [^{35}S]methionine and incubated with GST or GST–TAp63alpha deletion mutants at 4 °C for 2 h. After the addition of 30 μl glutathione-Sepharose beads to the reaction mixture, incubation was continued at 4 °C for 1 h. The beads were collected by centrifugation and washed three times with binding buffer containing 50 mM Tris-HCl (pH 7.5), 150 mM NaCl, 0.1% Nonidet P-40 and 1 mM EDTA. The ^{35}S-labeled-bound proteins were eluted using 2 × SDS sample buffer and separated by 10% SDS–PAGE. After electrophoresis, the gel was dried and exposed to X-ray film with an intensifying screen.

Flow cytometry
After transfection, both floating and attached cells were collected by low-speed centrifugation and washed in phosphate-buffered saline. The cells were then stained with propidium iodide (50 μg/ml) in the presence of 50 μg/ml of RNase A for 30 min at room temperature. The DNA content indicated by propidium iodide staining was analysed using a FACSCalibur flow cytometer (BD Biosciences, San Jose, CA, USA).

Luciferase reporter assay
Luciferase reporter assay was carried out as described earlier (Koida *et al*., 2008). Each experiment was carried out at least three times in triplicate.

In vitro *kinase assay*
To identify the possible Ser residue(s) of TAp63alpha that could be phosphorylated by Plk1, we carried out *in vitro* kinase assay according to the previous report (Koida *et al*., 2008). In brief, GST–TAp63alpha-(1–102), GST-S41A and GST-S52A were incubated with the active form of Plk1 (cat no. CY-E1163, CycLex, Nagano, Japan) in the presence of 10 μCi of [γ-^{32}P]ATP (~6000 Ci/mmol, GE Healthcare) in 40 μl of kinase buffer (40 mM HEPES (4-(2-hydroxyethyl)-1-piperazineethanesulfonic acid), 10 mM $MgCl_2$, 1 mM dithiotreitol and 3 mM $MnCl_2$). Reactions were incubated at 30 °C for 30 min and terminated by the addition of Laemmli SDS sample dilution buffer. The reaction mixtures were separated by SDS–PAGE and subjected to autoradiography.

RNA interference
To knockdown endogenous Plk1, TAp63 and p73, cells were transiently transfected with the chemically synthesized siRNA targeting Plk1, TAp63 and p73 or with the control siRNA using Lipofectamine RNAiMAX (Invitrogen) according to the manufacturer's recommendations. Total RNA and whole-cell lysates were prepared 48 h after transfection. The specific sequences were as follows: Plk1, 5′-AACCAGUGGUUCGAGAGACAG-3′; TAp63, 5′-GAUGGUGCGACAAACAAGA-3′; and p73, 5′-CGGAUUCCAGCAUGGACGU-3′. Selected siRNA sequences were submitted to a BLAST search against the human genome sequence to ensure specificity. *Silencer* Negative Control #1 siRNA (Ambion, Austin, TX, USA) was used as control siRNA.

Construction of the deletion mutants of Plk1
For construction of the deletion mutants of Plk1, pcDNA3-FLAG-*Plk1* was digested with *Bam*HI, *Bam*HI/*Bst*XI and *Bam*HI/*Nco*I for the fragments encoding amino acid residues 1–401, 1–329 and 1–98, respectively. These fragments were purified from agarose gels, filled in the overhangs with Klenow enzyme and then inserted in-frame into enzymatically modified *Bam*HI and *Xho*I sites of the pcDNA3-FLAG expression plasmid to obtain pcDNA3-FLAG-*Plk1*-(1–401), pcDNA3-FLAG-*Plk1*-(1–329), and pcDNA3-FLAG*Plk1*-(1–98), respectively. DNA sequencing confirmed the authenticity of the expression plasmids before transfection.

Acknowledgements

We thank K Sakurai for technical assistance and Daniel Mrozek, Medical English Service, for editorial assistance. This work was supported, in part, by a grant-in-aid from the Ministry of Health, Labor, and Welfare for Third Term Comprehensive Control Research for Cancer; a grant-in-aid for Cancer Research (20-13) from the Ministry of Health, Labor, and Welfare of Japan; and a grant-in-aid from the Ministry of Education, Culture, Sports, Science and Technology, Japan.

References

Ando K, Ozaki T, Yamamoto H, Furuya K, Hosoda M, Hayashi S *et al*. (2004). Polo-like kinase 1 (Plk1) inhibits p53 function by physical interaction and phosphorylation. *J Biol Chem* **279**: 25549–25561.

Blandino G, Dobbelstein M. (2004). p73 and p63: why do we still need them? *Cell Cycle* **3**: 886–894.

Bruix J, Llovet JM. (2002). Prognostic prediction and treatment strategy in hepatocellular carcinoma. *Hepatology* **35**: 519–524.

Candi E, Dinsdale D, Rufini A, Salomoni P, Knight RA, Mueller M *et al*. (2007). TAp63 and DeltaNp63 in cancer and epidermal development. *Cell Cycle* **6**: 274–285.

Candi E, Terrinoni A, Rufini A, Chikh A, Lena AM, Suzuki Y *et al.* (2006). p63 is upstream of IKK alpha in epidermal development. *J Cell Sci* **119**: 4617–4622.

Chiba T, Kita K, Zheng YW, Yokosuka O, Saisho H, Iwama A *et al.* (2006). Side population purified from hepatocellular carcinoma cells harbors cancer stem cell-like properties. *Hepatology* **44**: 240–251.

Eckerdt F, Strebhardt K. (2006). Polo-like kinase 1: target and regulator of anaphase-promoting complex/cyclosome-dependent proteolysis. *Cancer Res* **66**: 6895–6898.

Flores ER, Tsai KY, Crowley D, Sengupta S, Yang A, McKeon F *et al.* (2002). p63 and p73 are required for p53-dependent apoptosis in response to DNA damage. *Nature* **416**: 560–564.

Ghioni P, D'Alessandra Y, Mansueto G, Jaffray E, Hay RT, La Mantia G *et al.* (2005). The protein stability and transcriptional activity of p63alpha are regulated by SUMO-1 conjugation. *Cell Cycle* **4**: 183–190.

Gressner O, Schilling T, Lorenz K, Schulze Schleithoff E, Koch A, Schulze-Bergkamen H *et al.* (2005). TAp63alpha induces apoptosis by activating signaling via death receptors and mitochondria. *EMBO J* **24**: 2458–2471.

Huang YP, Wu G, Guo Z, Osada M, Fomenkov T, Park HL *et al.* (2004). Altered sumoylation of p63alpha contributes to the split-hand/foot malformation phenotype. *Cell Cycle* **3**: 1587–1596.

Ichikawa T, Suenaga Y, Koda T, Ozaki T, Nakagawara A. (2008). TAp63-dependent induction of growth differentiation factor 15 (GDF15) plays a critical role in the regulation of keratinocyte differentiation. *Oncogene* **27**: 409–420.

Kato S, Shimada A, Osada M, Ikawa S, Obinata M, Nakagawara A *et al.* (1999). Effects of p51/p63 missense mutations on transcriptional activities of p53 downstream gene promoters. *Cancer Res* **59**: 5908–5911.

Koga F, Kawakami S, Fujii Y, Saito K, Ohtsuka Y, Iwai A *et al.* (2003). Impaired p63 expression associates with poor prognosis and uroplakin III expression in invasive urothelial carcinoma of the bladder. *Clin Cancer Res* **9**: 5501–5507.

Koida N, Ozaki T, Yamamoto H, Ono S, Koda T, Ando K *et al.* (2008). Inhibitory role of Plk1 in the regulation of p73-dependent apoptosis through physical interaction and phosphorylation. *J Biol Chem* **283**: 8555–8563.

Koster MI, Kim S, Mills AA, DeMayo FJ, Roop DR. (2004). p63 is the molecular switch for initiation of an epithelial stratification program. *Genes Dev* **18**: 126–131.

Levine AJ. (1997). p53, the cellular gatekeeper for growth and division. *Cell* **88**: 323–331.

Lu LY, Wood JL, Minter-Dykhouse K, Ye L, Saunders TL, Yu X *et al.* (2008). Polo-like kinase 1 is essential for early embryonic development and tumor suppression. *Mol Cell Biol* **28**: 6870–6876.

MacPartlin M, Zeng SX, Lu H. (2008). Phosphorylation and stabilization of TAp63gamma by IkappaB kinase-beta. *J Biol Chem* **283**: 15754–15761.

Massion PP, Taflan PM, Jamshedur Rahman SM, Yildiz P, Shyr Y, Edgerton ME *et al.* (2003). Significance of p63 amplification and overexpression in lung cancer development and prognosis. *Cancer Res* **63**: 7113–7121.

Mills AA, Zheng B, Wang XJ, Vogel H, Roop DR, Bradley A. (1999). p63 is a p53 homologue required for limb and epidermal morphogenesis. *Nature* **398**: 708–713.

Moll UM, Slade N. (2004). p63 and p73: roles in development and tumor formation. *Mol Cancer Res* **2**: 371–386.

Montesano R, Hainaut P, Wild CP. (1997). Hepatocellular carcinoma: from gene to public health. *J Natl Cancer Inst* **89**: 1844–1851.

Nakajima H, Toyoshima-Morimoto F, Taniguchi E, Nishida E. (2003). Identification of a consensus motif for Plk (Polo-like kinase) phosphorylation reveals Myt1 as a Plk1 substrate. *J Biol Chem* **278**: 25277–25280.

Nguyen BC, Lefort K, Mandinova A, Antonini D, Devgan V, Della Gatta G *et al.* (2006). Cross-regulation between Notch and p63 in keratinocyte commitment to differentiation. *Genes Dev* **20**: 1028–1042.

Parkin DM, Bray F, Ferlay J, Pisani P. (2001). Estimating the world cancer burden: Globocan 2000. *Int J Cancer* **94**: 153–156.

Petitjean A, Cavard C, Shi H, Tribollet V, Hainaut P, Caron de Fromentel C. (2005). The expression of TA and DeltaNp63 are regulated by different mechanisms in liver cells. *Oncogene* **24**: 512–519.

Rocco JW, Leong CO, Kuperwasser N, DeYoung MP, Ellisen LW. (2006). p63 mediates survival in squamous cell carcinoma by suppression of p73-dependent apoptosis. *Cancer Cell* **9**: 45–56.

Sasaki Y, Ishida S, Morimoto I, Yamashita T, Kojima T, Kihara C *et al.* (2002). The p53 family member genes are involved in the Notch signal pathway. *J Biol Chem* **277**: 719–724.

Shen HM, Ong CN. (2004). Mutations of the p53 tumor suppressor gene and ras oncogenes in aflatoxin hepatocarcinogenesis. *Mutat Res* **366**: 23–44.

Shieh SY, Ikeda M, Taya Y, Prives C. (1997). DNA damage-induced phosphorylation of p53 alleviates inhibition by MDM2. *Cell* **91**: 325–334.

Smits VA, Klompmaker R, Arnaud L, Rijksen G, Nigg EA, Medema RH. (2000). Polo-like kinase-1 is a target of the DNA damage checkpoint. *Nat Cell Biol* **2**: 672–676.

Strebhardt K, Ullrich A. (2006). Targeting polo-like kinase 1 for cancer therapy. *Nat Rev Cancer* **6**: 321–330.

Suh EK, Yang A, Kettenbach A, Bamberger C, Michaelis AH, Zhu Z *et al.* (2006). p63 protects the female germ line during meiotic arrest. *Nature* **444**: 624–628.

Urist MJ, Di Como CJ, Lu ML, Charytonowicz E, Verbel D, Crum CP *et al.* (2002). Loss of p63 expression is associated with tumor progression in bladder cancer. *Am J Pathol* **161**: 1199–1206.

van Vugt MA, Smits VA, Klompmaker R, Medema RH. (2001). Inhibition of Polo-like kinase-1 by DNA damage occurs in an ATM- or ATR-dependent fashion. *J Biol Chem* **276**: 41656–41660.

Vousden KH, Lu X. (2002). Live or let die: the cell's response to p53. *Nat Rev Cancer* **2**: 594–604.

Westfall MD, Joyner AS, Barbieri CE, Livingstone M, Pietenpol JA. (2005). Ultraviolet radiation induces phosphorylation and ubiquitin-mediated degradation of DeltaNp63alpha. *Cell Cycle* **4**: 710–716.

Westfall MD, Mays DJ, Sniezek JC, Pietenpol JA. (2003). The Delta Np63 alpha phosphoprotein binds the p21 and 14-3-3 sigma promoters *in vivo* and has transcriptional repressor activity that is reduced by Hay–Wells syndrome-derived mutations. *Mol Cell Biol* **23**: 2264–2276.

Winkles JA, Alberts GF. (2005). Differential regulation of polo-like kinase 1, 2, 3, and 4 gene expression in mammalian cells and tissues. *Oncogene* **24**: 260–266.

Yamada S, Ohira M, Horie H, Ando K, Takayasu H, Suzuki Y *et al.* (2004). Expression profiling and differential screening between hepatoblastomas and the corresponding normal livers: identification of high expression of the PLK1 oncogene as a poor-prognostic indicator of hepatoblastomas. *Oncogene* **23**: 5901–5911.

Yang A, Kaghad M, Wang Y, Gillett E, Fleming MD, Dötsch V *et al.* (1998). p63, a p53 homolog at 3q27-29, encodes multiple products with transactivating, death-inducing, and dominant-negative activities. *Mol Cell* **2**: 305–316.

Yang A, Schweitzer R, Sun D, Kaghad M, Walker N, Bronson RT *et al.* (1999). p63 is essential for regenerative proliferation in limb, craniofacial and epithelial development. *Nature* **398**: 714–718.

Zhou J, Zhang Y. (2008). Cancer stem cells: models, mechanisms and implications for improved treatment. *Cell Cycle* **7**: 1360–1370.

Supplementary Information accompanies the paper on the Oncogene website (http://www.nature.com/onc)

THE JOURNAL OF BIOLOGICAL CHEMISTRY VOL. 284, NO. 48, pp. 33185–33194, November 27, 2009

Reactive Oxygen Species-generating Mitochondrial DNA Mutation Up-regulates Hypoxia-inducible Factor-1α Gene Transcription via Phosphatidylinositol 3-Kinase-Akt/Protein Kinase C/Histone Deacetylase Pathway*[S]

Received for publication, August 13, 2009, and in revised form, September 20, 2009 Published, JBC Papers in Press, October 1, 2009, DOI 10.1074/jbc.M109.054221

Nobuko Koshikawa[‡], **Jun-Ichi Hayashi**[§], **Akira Nakagawara**[¶1], **and Keizo Takenaga**[‡‖2]

From the [‡]*Laboratory of Cancer Metastasis and* [¶]*Division of Biochemistry and Innovative Cancer Therapeutics, Chiba Cancer Center Research Institute, 666-2 Nitona, Chuoh-ku, Chiba 260-8717, the* [§]*Graduate School of Life and Environmental Sciences, University of Tsukuba, 1-1-1 Tennodai, Tsukuba, Ibaraki 305-8572, and the* [‖]*Laboratory of Tumor Biology, Division of Life Science, Shimane University Faculty of Medicine, 89-1 Enya, Izumo, Shimane 693-8501, Japan*

Lewis lung carcinoma-derived high metastatic A11 cells constitutively overexpress hypoxia-inducible factor (HIF)-1α mRNA compared with low metastatic P29 cells. Because A11 cells exclusively possess a G13997A mutation in the mitochondrial NADH dehydrogenase subunit 6 (*ND6*) gene, we addressed here a causal relationship between the *ND6* mutation and the activation of *HIF-1α* transcription, and we investigated the potential mechanism. Using trans-mitochondrial cybrids between A11 and P29 cells, we found that the *ND6* mutation was directly involved in *HIF-1α* mRNA overexpression. Stimulation of *HIF-1α* transcription by the *ND6* mutation was mediated by overproduction of reactive oxygen species (ROS) and subsequent activation of phosphatidylinositol 3-kinase (PI3K)-Akt and protein kinase C (PKC) signaling pathways. The up-regulation of *HIF-1α* transcription was abolished by mithramycin A, an Sp1 inhibitor, but luciferase reporter and chromatin immunoprecipitation assays indicated that Sp1 was necessary but not sufficient for *HIF-1α* mRNA overexpression in A11 cells. On the other hand, trichostatin A, a histone deacetylase (HDAC) inhibitor, markedly suppressed *HIF-1α* transcription in A11 cells. In accordance with this, HDAC activity was high in A11 cells but low in P29 cells and in A11 cells treated with the ROS scavenger ebselene, the PI3K inhibitor LY294002, and the PKC inhibitor Ro31-8220. These results suggest that the ROS-generating *ND6* mutation increases *HIF-1α* transcription via the PI3K-Akt/PKC/HDAC pathway, leading to HIF-1α protein accumulation in hypoxic tumor cells.

Somatic mutations in mitochondrial DNA (mtDNA) have been shown to accumulate in cancer cells and proposed to contribute to the progression of cancers of a variety of tissue origins. Mitochondria are the key regulators of the oxidative phosphorylation system that is composed of five complexes (I–V). Some somatic mtDNA mutations are envisioned as inhibiting the electron transport chain, resulting in a marked increase in mitochondrial reactive oxygen species (ROS)[3] production (1). Actually, for example, a heteroplasmic frameshift mtDNA mutation in the NADH dehydrogenase subunit 5 (*ND5*) gene and a deletion mutant of cytochrome B (*CYTB*) gene promote ROS generation (2, 3). In addition, we have recently reported that a missense mutation in the *ND6* gene causes the reduction of complex I activity, ROS overproduction, and increased metastatic potential of Lewis lung carcinoma cells (4).

Hypoxia is a common characteristic of locally advanced solid tumors. Hypoxic tumor cells activate many genes, including those related to cell survival, glycolysis, and angiogenesis, and invasion and metastasis to adapt to and escape from the microenvironment (5, 6). The oxygen-sensing mechanisms have been studied extensively and revealed hypoxia-inducible factors (HIFs) as the key regulatory transcription factors that are composed of HIF-α subunit and HIF-β/ARNT subunit. Under normoxic conditions, the α subunit (HIF-1α) is hydroxylated at Pro^{564} and Pro^{402} by specific Fe^{2+}, oxoglutarate, and oxygen-dependent prolyl hydroxylases, recognized and ubiquitinated by an E3 ubiquitin ligase complex consisting of the tumor suppressor VHL (von Hippel-Lindau), elongin B and elongin C, and rapidly degraded through the ubiquitin-proteasome pathway, whereas the β subunit of HIF-1 (HIF-1β) is constitutively expressed. Under hypoxic conditions, HIF-1α protein is stabilized, allowing its nuclear translocation and dimerization with HIF-1β. In the nucleus, HIF binds to the hypoxia response element of hypoxia-inducible genes, including vascular endothe-

* This work was supported in part by Grants-in-aid for Third Term Comprehensive Control Research for Cancer from the Ministry of Health, Labor, and Welfare (to K. T.) and by Grants-in-aid for Scientific Research from the Ministry of Education, Culture, Sports, Science, and Technology of Japan (to N. K. and K. T.).

[S] The on-line version of this article (available at http://www.jbc.org) contains supplemental Figs. S1–S3 and Table S1.

[1] To whom correspondence may be addressed: 666-2 Nitona, Chuoh-ku, Chiba 260-8717, Japan. Fax: 81 43 265 4459; E-mail: akiranak@chiba-cc.jp.

[2] To whom correspondence may be addressed: 89-1 Enya, Izumo, Shimane 693-8501, Japan. Fax: 81 853 20 2340; E-mail: biokeizo@med.shimane-u.ac.jp.

[3] The abbreviations used are: ROS, reactive oxygen species; DCFH-DA, 2′,7′-dichlorofluorescin diacetate; DMEM, Dulbecco's modified Eagle's medium; DPBS, Dulbecco's phosphate-buffered saline; EMSA, electrophoretic mobility shift assay; ERK, extracellular signal-regulated kinase; FACS, fluorescence-activated cell sorter; HDAC, histone deacetylase; HIF-1α, hypoxia-inducible factor-1α; JNK, c-Jun N-terminal kinase; MAP, mitogen-activated protein; ND6, NADH dehydrogenase subunit 6; PDTC, pyrrolidine dithiocarbamate; PI3K, phosphatidylinositol 3-kinase; PKC, protein kinase C; PMSF, phenylmethylsulfonyl fluoride; TSA, trichostatin A; VEGF, vascular endothelial growth factor.

lial growth factor (VEGF), and transactivates their transcription (5, 6).

Elevated HIF-1α protein levels are commonly observed in many tumor tissues and associated with increased angiogenesis, resistance to apoptosis and chemo- and radiotherapy, and poor patient prognosis (6, 7). Hypoxia generated by aberrant vasculature formation and high interstitial pressure is undoubtedly a major factor, but other factors such as activation of *HIF-1α* gene transcription may also play a role in up-regulation of HIF-1α protein in tumor tissues. Actually, we and others have reported the up-regulation of *HIF-1α* mRNA in some tumor types (8–10). Although the precise mechanism of *HIF-1α* gene activation is largely unknown, an increase in gene dosage is reported as one of the mechanisms of constitutive up-regulation of *HIF-1α* mRNA expression (9, 10).

ROS are the physiological mediators to stabilize and increase the transcriptional activity of HIF-1α protein. Incubation of cells with H_2O_2 or an oxidative stressor leads to the stabilization of HIF-1α protein and activation of HIF target genes under normoxic conditions (11). Conversely, treatment of cells with antioxidants such as *N*-acetylcysteine and glutathione attenuates HIF-1α protein accumulation and the expressions of HIF target genes in various cell types (11). HIF-1α protein levels increase under normoxia in response to growth factors, hormones, coagulation factors, cytokines, and vasoactive peptides, which also stimulate ROS generation (12, 13). Mitochondria-derived ROS produced by electron transport chain complex III are also reported to be able to stabilize HIF-1α protein under hypoxic conditions (14). Although the stabilization of HIF-1α protein by ROS has been highlighted, *HIF-1α* mRNA expression is also stimulated by ROS from NADPH oxidase (15).

So far, there are no reports of the involvement of mtDNA mutations in the activation of the *HIF-1α* gene. Given a high frequency of mtDNA mutation rate in tumor cells and ROS-mediated HIF-1α accumulation at both the protein and mRNA levels, we reasoned that mtDNA mutations could be a cause of *HIF-1α* transcriptional activation. In the present study, we addressed this issue and investigated the potential mechanism. We report here that certain ROS-generating mtDNA mutations can stimulate *HIF-1α* transcription via the phosphatidylinositol 3-kinase (PI3K)/protein kinase C (PKC)/histone deacetylase (HDAC) pathway.

EXPERIMENTAL PROCEDURES

Reagents—Actinomycin D was purchased from Sigma-Aldrich; and SB203580, LY294002, Ro31-8220, ebselene, pyrrolidine dithiocarbamate (PDTC), trichostatin A (TSA), mithramycin A, sulfasarazine, and curcumin were from Calbiochem. SP600125 was obtained from TOCRIS Cookson, Ellisville, MO, and PD98059 was from Cell Signaling Technology, Beverly, MA.

Antibodies—Monoclonal anti-HIF-1α antibody was obtained from Novus Biologicals, Littleton, CO. Polyclonal anti-p38 MAP kinase, anti-phospho-p38 MAP kinase (Thr^{180}/Tyr^{182}), anti-p44/42 MAP kinase, anti-phospho-p44/42 MAP kinase (Thr^{202}/Tyr^{185}), anti-SAPK/JNK, anti-phospho-SAPK/JNK (Thr^{183}/Tyr^{185}), anti-Akt, and anti-phospho-Akt (Ser^{473}), were purchased from Cell Signaling Technology. Polyclonal anti-Sp1, anti-Sp3, anti-E2F-1 antibodies and normal rabbit IgG were obtained from Santa Cruz Biotechnology, monoclonal anti-β-actin antibody was from Sigma-Aldrich, and polyclonal anti-acetylhistone H4 antibody was from Upstate, Charlottesville, VA.

Cell Lines and Culture Conditions—Low metastatic P29 and P34 cells and high metastatic D6 and A11 cells, all of which were derived from Lewis lung carcinoma, were characterized previously (4, 8, 16). Trans-mitochondrial cybrids were established as described previously (4). P29mtA11 cybrids carry nuclear DNA from P29 cells and mtDNA from A11 cells, and A11mtP29 cybrids carry nuclear DNA from A11 cells and mtDNA from P29 cells. As controls, P29mtP29 cybrids, which have nuclear DNA from P29 cells and mtDNA from P29 cells, and A11mtA11 cybrids, which have nuclear DNA from A11 cells and mtDNA from A11 cells, were used. Lewis lung carcinoma cells were maintained in Dulbecco's modified Eagle's medium (DMEM) supplemented with heat-inactivated (56 °C, 30 min) fetal bovine serum, 100 units/ml penicillin, and 100 μg/ml streptomycin. Trans-mitochondrial cybrids were maintained in DMEM supplemented with heat-inactivated fetal bovine serum, 100 units/ml penicillin, 100 μg/ml streptomycin, 0.01% pyruvate, and 0.005% uridine. For hypoxic culture, they were incubated under hypoxic conditions (1% O_2) in a NAPCO® automatic O_2/CO_2 incubator (Precision Scientific, Chicago, IL).

Sequencing of the ND6 Gene—Total DNAs extracted from P29, P34, D6, and A11 cells were used for amplification of the *ND6* gene. The primers used for PCRs were as follows: the forward primer (n.p. 14,030 to 14,053, 5′-CAATTTCACAGCACCAAATCTCCA-3′) and the reverse primer (n.p. 14,759 to 14,779, 5′-TATTAGGGGGTTAGTTTTGCG-3′). All PCR amplifications were performed in a 50 μl of solution consisting of 1× PCR buffer, 0.2 mM dinucleotide triphosphates, 0.6 μM primers, 1 unit of *ExTaq* DNA polymerase (TaKaRa BIO, Shiga, Japan), and 10 ng of genomic DNA as a template. Reaction conditions were 94 °C for 1 min with cycle times of 30 s for denaturation at 94 °C, 30 s for annealing at 53 °C, and 1 min for extension at 72 °C for 30 cycles. The final extension was for 1 min. Amplified *ND6* fragments were separated on 1% agarose gels and extracted and then directly sequenced using a Big Dye Terminator version 3.1 cycle sequencing kit (Applied Biosystems).

Measurement and Visualization of ROS Generation—ROS generation was detected with 2′,7′-dichlorofluorescin diacetate (DCFH-DA) (Molecular Probes, Eugene, OR). Briefly, the cells cultured in 35-mm-diameter glass-bottom culture dishes (MatTeck, Ashland, MA) were incubated with 10 μM DCFH-DA for 10 min at 37 °C in serum-free DMEM, washed twice with Dulbecco's phosphate-buffered saline (DPBS), and then immediately observed under a confocal laser microscope (Fluoview; Olympus, Tokyo) or analyzed with a FACScan flow cytometer (Beckton Dickinson). Mean fluorescence intensity was analyzed using CellQuest software (Becton Dickinson).

RNA Isolation and Northern Blotting—Total RNA was extracted with guanidinium thiocyanate. Total RNA (20 μg) was electrophoresed on 1% agarose gels containing formaldehyde and transferred onto nylon filters. Blots were hybridized

with a ^{32}P-labeled mouse *HIF-1α* cDNA probe or a mouse *VEGF* cDNA probe (8), which was prepared by the random primer method. Filters were finally washed at 50 °C in 30 mM NaCl, 3 mM sodium citrate, and 0.1% SDS.

SDS-PAGE and Western Blotting—Total cell lysates were prepared by directly solubilizing cells in SDS sample buffer. For analyzes of phosphorylated proteins, cells were lysed in 1% Nonidet P-40, 150 mM NaCl, 10% glycerol, 2 mM EDTA, 20 mM Tris-HCl (pH 8.0), 1 mM dithiothreitol, 1 mM Na_3VO_4, 1 mM phenylmethylsulfonyl fluoride (PMSF), and protease inhibitor mixture (Roche Applied Science). Nuclear extracts were prepared using a nuclear extraction kit (Active Motif, Carlsbad, CA) according to the manufacturer's protocol. Proteins were resolved by SDS-PAGE under reducing conditions. Protein concentration was determined by the method of Bradford using bovine serum albumin as a standard. The resolved proteins were transferred electrophoretically to nitrocellulose membrane. After incubating with 5% dry milk in TBS-T (150 mM NaCl, 50 mM Tris-HCl (pH 7.4), 0.05% Tween 20) for at least 1 h at room temperature, the membrane was incubated with polyclonal or monoclonal antibody for the appropriate time, washed extensively with TBS-T, and then incubated with horseradish peroxidase-conjugated goat anti-rabbit or anti-mouse IgG, respectively. Proteins were detected using ECL Western blotting detection reagents (Amersham Biosciences).

Luciferase Reporter Plasmid Construction—Murine *HIF-1α* promoter from nucleotide −1958 to +93 (the transcriptional start site was defined as +1) inserted in the KpnI/SacI site of a luciferase reporter plasmid pGL2-basic, hereafter termed pGL2-HIFpro(−1958/+93), was a generous gift of Dr. C. A. Bradfield, University of Wisconsin Medical School (17). Various truncated forms of the promoter were made by utilizing restriction enzyme recognition sites in the promoter and the vector (XbaI, KpnI/BbrPI, and SacII for making pGL2-HIFpro(−1422/+93), pGL2-HIFpro(−293/+93), and pGL2-HIFpro(−150/+93), respectively) or by PCR using the 5′ primers carrying the KpnI site at the 5′ end and the 3′ primer carrying SacI site at the 3′ end, 5′-GGGAGCTCCGGCTCGGGTTC-3′. The 5′ primers are: 5′-GAGGTACCTCAAGGTCTGTAGGTTGA-3′ for pGL2-HIFpro (−1048/+93), 5′-GAGGTACCATAGCAAAGAGCGGAGAC-3′ for pGL2-HIFpro(−668/+93), 5′-GAGGTACCTTTCCCTCCCCTCGCCGC-3′ for pGL2-HIFpro(−101/+93), and 5′-GAGGTACCCTTCAGCGCCTCAGTGCA-3′ for pGL2-HIFpro(−38/+93). The amplified PCR products were inserted into the KpnI/SacI site of a pGL2-basic vector. A pGL2-HIFpro(−150/+93)mutSp1 plasmid that harbors a mutation in the putative Sp1 binding site was generated by using the QuikChange Site-directed Mutagenesis kit (Stratagene, La Jolla, CA). The sense and the antisense primers used were 5′-CGCCCTTGCCCGAACCCTGCCGCTGC-3′ and 5′-GCAGCGGCAGGGTTCGGGCAAGGGCG-3′, respectively.

Luciferase Reporter Assay—Transient transfection of the luciferase reporter constructs harboring the *HIF-1α* promoter sequence was carried out using Lipofectamine Plus (Invitrogen). As a control for transfection efficiency, pRL-TK vector (Promega, Madison, WI) was cotransfected with test plasmids. pGL2-control vector (Promega) was used as a positive control. Luciferase activity in cell extracts was assayed 45 h after transfection according to the Dual-Luciferase reporter assay system protocols (Promega) using a luminometer (model TD-20/20; Turner Designs, Sunnyvale, CA).

Electrophoretic Mobility Shift Assay (EMSA)—The nuclear protein fractions for EMSA were prepared as described above. Consensus Sp1 (wtSp1, 5′-ATTCGATCGG**GG**CGGGGCGAGC-3′) and mutant Sp1 (mutSp1, 5′-ATTCGATCG**TT**CGGGGCGAGC-3′) double-stranded oligonucleotides were purchased from Santa Cruz Biotechnology. The *HIF-1α* gene promoter-specific double-stranded oligonucleotide probe (positions −72 to −48) (wtHIFpro-Sp1) or its mutant form (mutHIFpro-Sp1) was prepared by annealing the sense 5′-CGCCTCCGCCCTTGCCCG**CC**CCCTG-3′ and the antisense 5′-CAGGGG**GG**CGGGCAAGGGCGGAGGCG-3′ oligonucleotides or the sense 5′-CGCCTCCGCCCTTGCCCG**AA**CCCTG-3′ and the antisense 5′-CAGGG**TT**CGGGCAAGGGCGGAGGCG-3′, respectively. The probes were labeled using [γ-^{32}P]ATP (Amersham Biosciences) and MEGALABEL™ kit (TaKaRa BIO). Five micrograms of nuclear protein, ^{32}P-labeled double-stranded probe (5000 cpm), 1 μg of poly(dI·dC), and 17 μl of binding buffer (20 mM Hepes (pH 7.9), 50 mM NaCl, 5% glycerol, 0.1 mM dithiothreitol) were mixed in a total volume of 20 μl. In competition assays, a 50-fold molar excess amount of unlabeled competitors was included in the reaction mixture. The mixture was incubated at room temperature for 30 min, then loaded on a 5% polyacrylamide gel in TGE buffer (50 mM Tris-HCl (pH 8.5), 380 mM glycine, 2 mM EDTA), and subjected to electrophoresis at 4 °C. The gel was dried and exposed to x-ray film at −70 °C. A supershift assay was performed using 10 μg of specific goat polyclonal anti-Sp1 or anti-Sp3 antibody.

Chromatin Immunoprecipitation Assay—Cells were fixed with 1% formaldehyde for 10 min at 37 °C, and the reaction was quenched by adding glycine to a final concentration of 125 mM. The cells were washed with DPBS containing 1 mM PMSF; centrifuged; swelled in 5 mM Hepes (pH 8.0), 85 mM KCl, 0.5% Nonidet P-40, 0.5 mM PMSF, 100 ng/ml leupeptin, 100 ng/ml aprotinin; incubated for 10 min on ice; and then lysed with a Dounce homogenizer. Nuclei were collected by centrifugation and resuspended in sonication buffer (1% SDS, 10 mM EDTA, 50 mM Tris-HCl (pH 8.0), 0.5 mM PMSF, 100 ng/ml leupeptin, 100 ng/ml aprotinin). The nuclei were sonicated on ice to an average length of 500 to 1000 bp and then centrifuged at 10,000 × *g* for 15 min at 4 °C. The chromatin solution was diluted 10-fold in chromatin immunoprecipitation dilution buffer (500 mM Tris-HCl (pH 8.0), 1670 mM NaCl, 11% Triton X-100, 1.1% sodium deoxycholate, 10 mM PMSF, 10 μg/ml leupeptin, 10 μg/ml aprotinin, 10 μg/ml pepstatin), precleared by the addition of protein A-Sepharose beads for 1 h at 4 °C. Precleared chromatin solution was incubated with 5 μg of anti-Sp1 antibody, anti-Sp3 antibody, or anti-acetylhistone H4 antibodies at 4 °C for 13 h. Normal rabbit IgG served as a control. Protein·DNA complexes were immunoprecipitated by protein A beads, and the cross-links were reversed by heating to 65 °C for 5 h. The DNA was recovered by phenol:chloroform extraction and precipitated by ethanol. Then, the association of Sp1, Sp3, and acetylated histone H4 with the Sp1/Sp3 recognition site in the *HIF-1α* promoter was examined by hot-start PCR

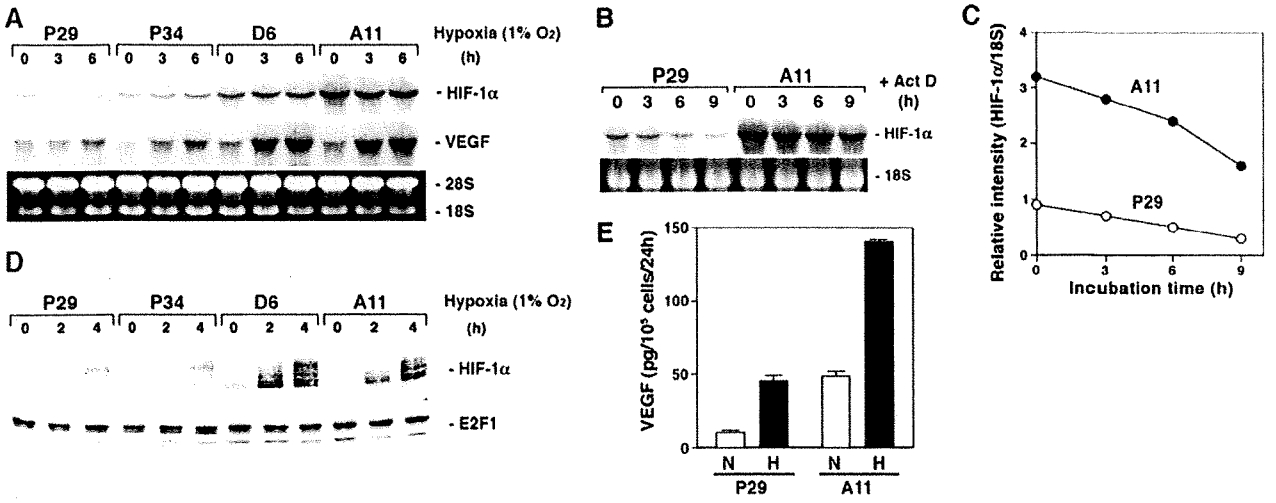

FIGURE 1. **HIF-1α and VEGF expressions are higher in high metastatic D6 and A11 cells than in low metastatic P29 and P34 cells.** *A*, P29, P34, D6, and A11 cells were cultured under hypoxic conditions (1% O_2) for up to 6 h. Total RNA was extracted and subjected to Northern blot analysis. The blots were hybridized with either a ^{32}P-labeled *HIF-1α* or *VEGF* cDNA probe. Ethidium bromide staining of the gel is also shown. *B* and *C*, P29 and A11 cells were incubated with 5 μg/ml actinomycin D (*Act D*) for up to 9 h. Total RNA was extracted and analyzed as above. Ethidium bromide staining of 18 S ribosomal RNA is also shown. After semiquantifying the intensities of bands, the levels of *HIF-1α* mRNA were normalized to those of 18 S ribosomal RNA. *D*, P29, P34, D6, and A11 cells were cultured under hypoxic conditions for up to 4 h. Nuclear extracts prepared from the cells were dissolved by SDS-PAGE. HIF-1α and E2F1, which served as a control, were detected by immunoblotting. *E*, P29 and A11 cells were cultured under normoxic (*N*) or hypoxic (*H*) conditions for 18 h. VEGF produced in the supernatants was measured by enzyme-linked immunosorbent assay. *Bars*, S.D.

using *GoTaq*DNA polymerase (Promega). The sense and the antisense primers used were 5′-ACCTCCTCCTGATTGGCTG-3′ (positions −258 to −239) and 5′-TCGCGTCCCCTCAGCCGA-3′ (positions −12 to +5), respectively. The PCR conditions were: 96 °C for 5 min, 30 cycles with 96 °C for 30 s, 57 °C for 30 s, and 72 °C for 30 s, and 72 °C for 5 min. Final PCR products were analyzed on 2% agarose gels with ethidium bromide staining.

CD31 Staining of Tumor Blood Vessels—P29mtP29, P29mtA11, A11mtA11, and A11mtP29 cells (1×10^6 cells) were inoculated subcutaneously into the abdominal flank of C57BL/6 mice. When an estimated tumor volume reached ~2 cm^3, subcutaneous tumors were surgically removed and immediately frozen in OCT compound. Cryostat sections (10-μm thickness) were made at every 100-μm distance, fixed with 4% paraformaldehyde, and then washed with DPBS. After blocking with 10% normal goat serum in DPBS, sections were incubated with rat anti-mouse CD31 antibody (1:100 dilutions) (BD Pharmingen) overnight at 4 °C. They were washed with DPBS and incubated with fluorescein isothiocyanate-conjugated goat anti-rat IgG. After extensive washing with DPBS, samples were counterstained with 1 μg/ml propidium iodide and observed under a confocal laser microscope (Fluoview). Images were captured and transferred to the ImageJ 1.34s software, and CD31-positive areas were analyzed. In this way, at least six randomly selected fields (0.2 cm^2/field) were analyzed, and the percentage of CD31-positive area per field was calculated.

HDAC Activity Assay—Nuclear extracts were prepared using a nuclear extraction kit. HDAC activity was measured using a HDAC fluorometric assay/drug discovery kit (BioMol International, Plymouth Meeting, PA) according to the manufacturer's instruction. Briefly, 4.5-μg nuclear extracts were incubated with Fluor de Lys substrate buffer at 37 °C for 30 min followed by incubation with Fluor de Lys developer concentrate at 25 °C for 10 min. Fluorescence was measured with a multiwell plate reader (excitation at 355 nm and emission at 460 nm).

RESULTS

Activation of HIF-1α Gene Transcription in High Metastatic Cells—We compared the expression level of *HIF-1α* mRNA between the low metastatic (P29 and P34) and the high metastatic (D6 and A11) cells originated from Lewis lung carcinoma. The results showed that D6 and A11 cells expressed a larger amount of *HIF-1α* mRNA than P29 and P34 cells (Fig. 1*A*). Hypoxia did not affect the expression level of the mRNA. One of the possible mechanisms of *HIF-1α* mRNA up-regulation in D6 and A11 cells may be the difference in *HIF-1α* mRNA stability in the cells. To test this possibility, we cultured P29 and A11 cells in the presence of actinomycin D for up to 9 h and examined the mRNA level at each time point (Fig. 1*B*). The results showed that the half-life of *HIF-1α* mRNA in A11 cells was nearly equal to that in P29 cells (~8 h) (Fig. 1*C*). Thus, the transcription of the *HIF-1α* gene was found to be more activated in A11 cells than in P29 cells.

Under normoxic conditions, HIF-1α protein was scarcely detected in both the low and the high metastatic cells. However, upon hypoxic exposure, HIF-1α protein level markedly increased in D6 and A11 cells compared with P29 and P34 cells (Fig. 1*D*). Accordingly, hypoxia enhanced the expression of VEGF in D6 and A11 cells more than in P29 and P34 cells at both the mRNA and protein levels (Fig. 1, *A* and *E*). Thus, the up-regulation of *HIF-1α* mRNA in D6 and A11 cells resulted in overexpression of HIF-1α under hypoxic conditions, leading to VEGF overexpression.

ND6 Mutation Activates HIF-1α Transcription—Sequencing of the *ND6* gene revealed that D6 and A11 cells harbored

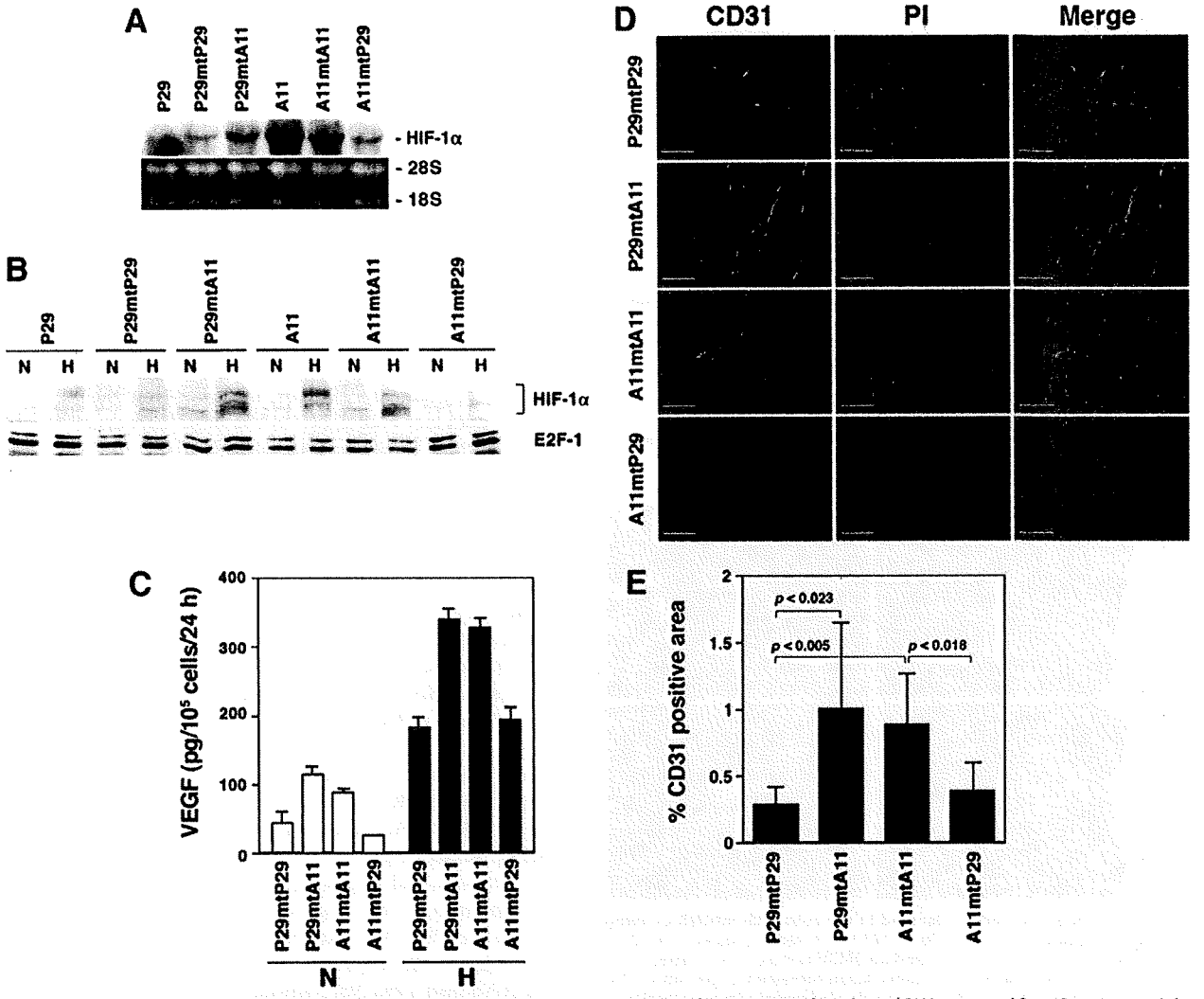

FIGURE 2. **HIF-1α and VEGF expressions are high in the cybrids with mtDNA carrying the *ND6* mutation.** *A*, total RNA extracted from P29, A11, and the cybrids was subjected to Northern blot analysis. The blots were hybridized with a ^{32}P-labeled *HIF-1α* cDNA. Ethidium bromide staining of the gel is also shown. *B*, P29 cells, A11 cells, and the cybrids were cultured under normoxic (*N*) or hypoxic (*H*) conditions for 4 h. Nuclear extracts prepared from the cells were dissolved by SDS-PAGE. HIF-1α and E2F1, which served as a control, were detected by immunoblotting. *C*, the cybrids were cultured under normoxic (*N*) or hypoxic (*H*) conditions for 18 h. VEGF produced in the supernatants was measured by enzyme-linked immunosorbent assay. *Bars*, S.D. *D*, cryostat sections prepared from subcutaneous tumors were stained with anti-CD31 antibody. Sections were counterstained with propidium iodide (*PI*). *E*, blood vessel density in subcutaneous tumors formed by the cybrids was assessed by staining with anti-CD31 antibody. The fluorescent images of at least six fields (0.2 cm^2/field) were analyzed, and the percentage of CD31-positive area/field (*columns*) was calculated. *Bars*, S.D.

a G13997A mutation, which changes evolutionally conserved proline 25 to leucine, whereas P29 and P34 cells did not (Fig. S1 and Table S1). To examine a causal relationship between the *ND6* mutation and *HIF-1α* transcription, we examined *HIF-1α* mRNA levels in trans-mitochondrial cybrids, P29mtA11 and A11mP29 cells, which carry mtDNA from A11 and P29 cells and nuclear DNA from P29 and A11 cells, respectively. We used P29mtP29 and A11mtA11 cells as control cybrids. The results showed that the expression level of *HIF-1α* mRNA was higher in the cybrids with A11 mtDNA (P29mtA11 and A11mtA11) irrespective of whether their nuclear DNA is derived from P29 or A11 cells, than in the cybrids with mtDNA from P29 cells (P29mtP29 and A11mtP29) (Fig. 2*A*). Accordingly, HIF-1α protein and VEGF were highly induced in P29mtA11 and A11mtA11 cybrids under hypoxic conditions compared with A11mtP29 and P29mtP29 cybrids (Fig. 2, *B* and *C*). Furthermore, P29mtA11 and A11mtA11 cybrids showed enhanced angiogenesis *in vivo* (Fig. 2, *D* and *E*). These results indicate that the *HIF-1α* mRNA overexpression in A11 and D6 cells is attributed to the *ND6* mutation.

ROS Are Involved in HIF-1α Transcriptional Activation by the ND6 Mutation—It is possible that mitochondrial ROS production caused by the *ND6* mutation mediates the activation of *HIF-1α* transcription. To examine this possibility, we measured the intracellular ROS level. Fluorescence-activated cell sorter (FACS) analysis and confocal images showed that D6 and A11 cells produced a larger amount of ROS than P29 and P34 cells (Fig. 3). In addition, the cybrids with mtDNA from A11 cells

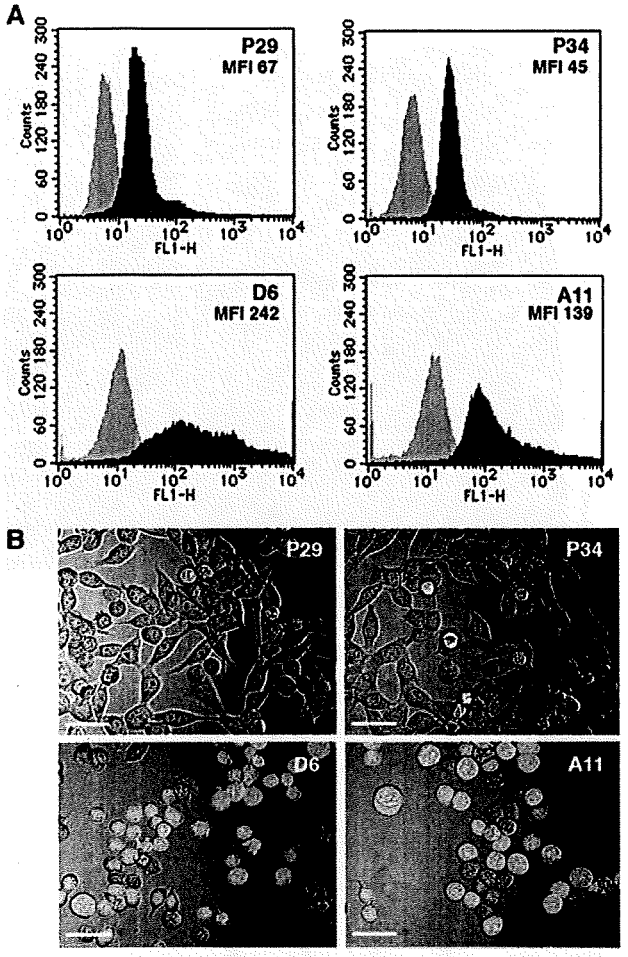

FIGURE 3. **ROS production is elevated in the cells with mtDNA carrying the *ND6* mutation.** *A*, P29, P34, D6, and A11 cells were incubated with 10 μM DCFH-DA for 10 min at 37 °C in serum-free DMEM and then immediately were analyzed with a FACScan flow cytometer. Mean fluorescence intensity (*MFI*) is also shown. *B*, the cells treated as above were observed under a confocal laser microscope.

(P29mtA11 and A11mtA11) overproduced ROS compared with the cybrids with mtDNA from P29 cells (P29mtP29 and A11mtP29) (Fig. S2). Thus, the *ND6* mutation is correlated well with both ROS overproduction and *HIF-1α* mRNA up-regulation.

Next, to gain evidence of a causal relationship between ROS and *HIF-1α* mRNA expression, we examined the effects of general antioxidants ebselene and PDTC, and antimycin A, which inhibits electron transport pathway (18). FACS analysis showed that intracellular ROS level was low in ebselene- and in PDTC-treated cells whereas high in antimycin A-treated cells compared with untreated cells, showing more distinct changes in A11 cells than in P29 cells (Fig. 4*A*). Ebselene and PDTC effectively suppressed the expression of *HIF-1α* mRNA in A11 cells, whereas antimycin A increased the expression in both P29 and A11 cells (Fig. 4*B*). These results strongly suggest that the *HIF-1α* transcriptional activation is regulated by mitochondrial ROS. Supporting this, we found that exogenously added H_2O_2 stimulated the expression of *HIF-1α* mRNA in P29 cells (Fig. 4*C*).

PI3K-Akt and PKC Signaling Pathways Are Involved in Mitochondrial ROS-mediated HIF-1α Overexpression—We next investigated signaling pathways of the mitochondrial ROS-mediated *HIF-1α* gene activation. For this, we treated P29 and A11 cells with PD98059, a MEK1 inhibitor, SB203580, a p38 MAP kinase inhibitor, SP600125, a JNK inhibitor, and LY294002, a PI3K inhibitor. As shown in Fig. 5*A*, LY294002 significantly inhibited *HIF-1α* mRNA expression in A11 cells in a dose-dependent manner, whereas PD98059, SB203580, and SP600125 did not, suggesting the involvement of the PI3K-Akt pathway in the mitochondrial ROS-mediated *HIF-1α* gene transcription. None of these inhibitors significantly suppressed *HIF-1α* mRNA expression in P29 cells, implying that the PI3K-Akt pathway does not contribute to the basal expression level of *HIF-1α* mRNA. In accordance with the data, Akt was highly activated, indicated by its protein phosphorylation, in D6 and A11 cells but not in P29 and P34 cells, and there was no consistent difference in the phosphorylation level of p38 MAP kinase, p44/42 MAP kinase, or JNK (Fig. 5*B*). Akt was also highly activated in P29mtA11 and A11mtA11 cybrids, but not in P29mtP29 and A11mtP29 cybrids (Fig. 5*C*). H_2O_2 strongly induced Akt activation in P29 cells in a time-dependent manner (Fig. 5*D*). Moreover, ebselene inhibited Akt phosphorylation in A11 cells (Fig. 5*E*). Thus, Akt phosphorylation is linked to the level of *HIF-1α* mRNA. In addition, Ro31-8220, a pan-specific PKC inhibitor, markedly inhibited *HIF-1α* mRNA expression in A11 cells, but only slightly in P29 cells, suggesting the involvement of PKC in the ROS-mediated *HIF-1α* mRNA expression (Fig. 5*F*). On the other hand, rapamycin, an mTOR inhibitor, sulfasarazine, an NF-κB inhibitor, and curcumin, an AP-1 inhibitor, did not significantly inhibit *HIF-1α* mRNA expression in A11 cells (Fig. S3). Collectively, these data indicate that the PI3K-Akt and PKC pathways are involved in the ROS-mediated *HIF-1α* transcriptional activation in A11 cells.

Sp1 Is Necessary but Not Sufficient for ROS-mediated HIF-1α Gene Activation—To gain further insight into the underlying mechanisms of *HIF-1α* gene activation in the high metastatic cell lines, we treated the cells with mithramycin A, an Sp1 inhibitor. The results showed that it significantly suppressed the expression of *HIF-1α* mRNA in D6 and A11 cells but not in P29 and P34 cells (Fig. 6*A*), suggesting the involvement of Sp1 in the ROS-mediated *HIF-1α* mRNA overexpression. To examine which region of the *HIF-1α* promoter is responsible for the activated transcription of the gene in A11 cells, we constructed luciferase reporter plasmids harboring the full-length (−1958/+93) and a series of truncated promoters (Fig. 6*B*). We transiently transfected them into A11 cells and examined their activities. The results showed that deletion of the region from −1958 to −101 effectively reduced the promoter activity compared with the full-length promoter, whereas deletion from −1958 to −150 did not significantly reduce the activity. Deletion of the region from −1958 to −38 abrogated the promoter activity, indicating that an important sequence for the promoter activity resides in the region from −149 to −38. Sequence analysis of this region using a computer software (TFSEARCH, Papia system) revealed a putative Sp1 binding

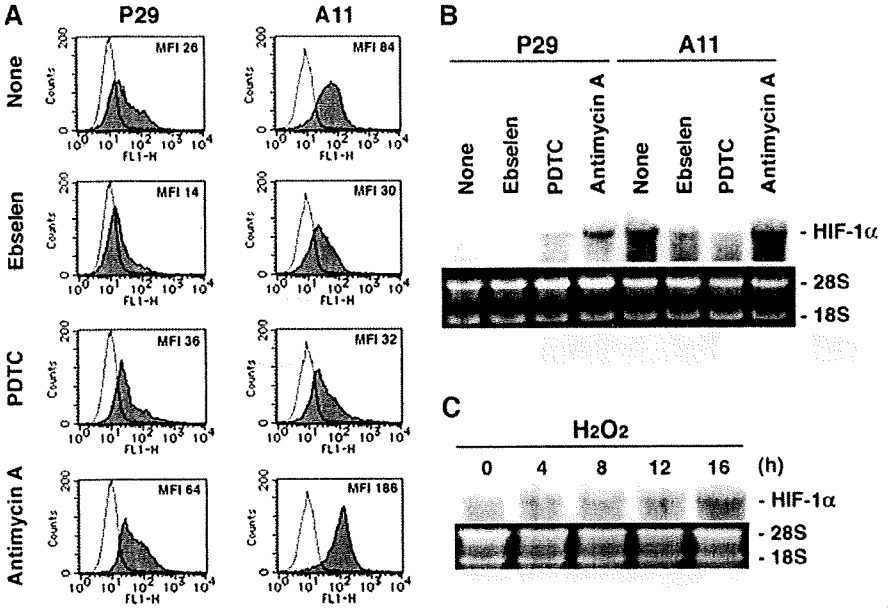

FIGURE 4. **ROS production is correlated with *HIF-1α* mRNA expression.** *A*, P29 and A11 cells were treated with solvent alone (dimethyl sulfoxide) (*None*), ebselen (20 μM), PDTC (20 μg/ml), and antimycin A (20 μg/ml) for 18 h. The cells were incubated with 10 μM DCFH-DA for 10 min at 37 °C in serum-free DMEM and then immediately were analyzed with a FACScan flow cytometer. Mean fluorescence intensity (*MFI*) is also shown. *B*, P29 and A11 cells were treated as above, and total extracted RNA was subjected to Northern blot analysis. The blots were hybridized with ^{32}P-labeled *HIF-1α* cDNA. Ethidium bromide staining of the gel is also shown. *C*, P29 cells were treated with 25 μM H_2O_2 for up to 16 h. Total extracted RNA was analyzed as in *B*.

sequence (−60/−51). Mutation of this sequence TGCCCGCCCC to TGCCCGAACC significantly reduced the promoter activity (Fig. 6*B*), demonstrating the importance of this sequence for the promoter activity.

To obtain direct evidence that Sp family members bind to this putative Sp1 binding sequence, we carried out EMSAs using wtHIFpro-Sp1 (−72/−48) as a DNA probe. As shown in Fig. 6*C*, these assays revealed three constitutive binding complexes (C1–C3) (*lane 2*) that were almost entirely Sp-dependent, as shown by competition with excess wtHIFpro-Sp1 or Sp1 consensus oligonucleotides (wtSp1) (*lanes 3* and *5*), but not with their mutant form mutHIFpro-Sp1 or mutSp1 (*lanes 4* and *6*). Addition of antibodies directed against either Sp1 or Sp3 induced a supershift and/or a significant reduction of Sp1/Sp3-dependent binding activities (*lanes 7* and *8*). Simultaneous addition of both antibodies led to a nearly complete supershift (*lane 9*). These data indicate that Sp1 and Sp3 proteins actually bind to the region proximal to the transcription initiation site.

We then compared the expression levels of Sp1 and Sp3 between the high and the low metastatic cell lines. However, we could not detect any difference (Fig. 6*D*). Also, the DNA binding activity of Sp1/Sp3, as demonstrated by EMSA analysis, did not correlate with the *HIF-1α* transcriptional level (Fig. 6*E*). Moreover, chromatin immunoprecipitation assays revealed that there were no differences in the binding of Sp1 and Sp3 to the Sp1/Sp3 binding site and the level of histone H4 acetylation around the site between P29 and A11 cells (Fig. 6*F*). These results indicate that Sp1 is necessary but not sufficient for explaining the higher expression of *HIF-1α* mRNA in the high metastatic cell lines.

HDAC Activation Contributes to the ROS-mediated HIF-1α Transcriptional Activation—To investigate a possible mechanism of the *HIF-1α* transcriptional activation in the high metastatic cells further, we treated P29 and A11 cells with TSA, a nonselective HDAC inhibitor. The results showed that TSA dramatically suppressed *HIF-1α* mRNA expression in A11 cells but slightly in P29 cells (Fig. 7*A*), suggesting the relationship between HDAC activity and the ROS-mediated *HIF-1α* mRNA overexpression. Then, we measured HDAC activity in P29 cells, P29 cells treated with H_2O_2, A11 cells, and A11 cells treated with ebselene, antimycin A, LY294002, and Ro31-8220. The results in Fig. 7*B* show that HDAC activity was significantly higher in A11 cells than in P29 cells. It was high in H_2O_2-treated P29 cells and antimycin A-treated A11 cells, but low in A11 cells treated with ebselene, LY294002, and Ro31-8220 compared with the respective untreated cells. Thus, the HDAC activity is positively correlated with the *HIF-1α* mRNA up-regulation.

DISCUSSION

The present study demonstrates that an ROS-generating mtDNA mutation in the *ND6* gene leads to *HIF-1α* mRNA overexpression, resulting in marked up-regulation of HIF-1α protein and VEGF production levels under hypoxic conditions. This study also suggests the possibility for the first time that some of pathogenic mtDNA mutations can activate *HIF-1α* transcription.

mtDNA mutations are frequently observed in tumor cells and implicated to be a factor in the progression of tumors. mtDNA mutations in tumor cells include severe mutations such as insertion-deletion and chain termination mutations and mild missense mutations. The mutation in the *ND6* gene found in A11 cells is a missense mutation that reduces complex I activity (4). This mutation was also found in the other high metastatic D6 cells but not in the low metastatic P29 or P34 cells. In both A11 and D6 cells, up-regulation of *HIF-1α* gene transcription was detected, suggesting a causal linkage between the *ND6* mutation and *HIF-1α* transcription. In the present study, we used trans-mitochondrial cybrids to prove this linkage, and as expected, the cybrids carrying mtDNA from A11 cells overexpressed *HIF-1α* mRNA, despite the source of nuclear DNA.

Several lines of evidence supported that ROS caused by the *ND6* mutation primarily mediates *HIF-1α* transcription. First, the cells carrying A11 mtDNA overproduced ROS. Second, ebselene and PDTC reduced the intracellular ROS level and concomitantly abolished *HIF-1α* transcription. Third, antimy-

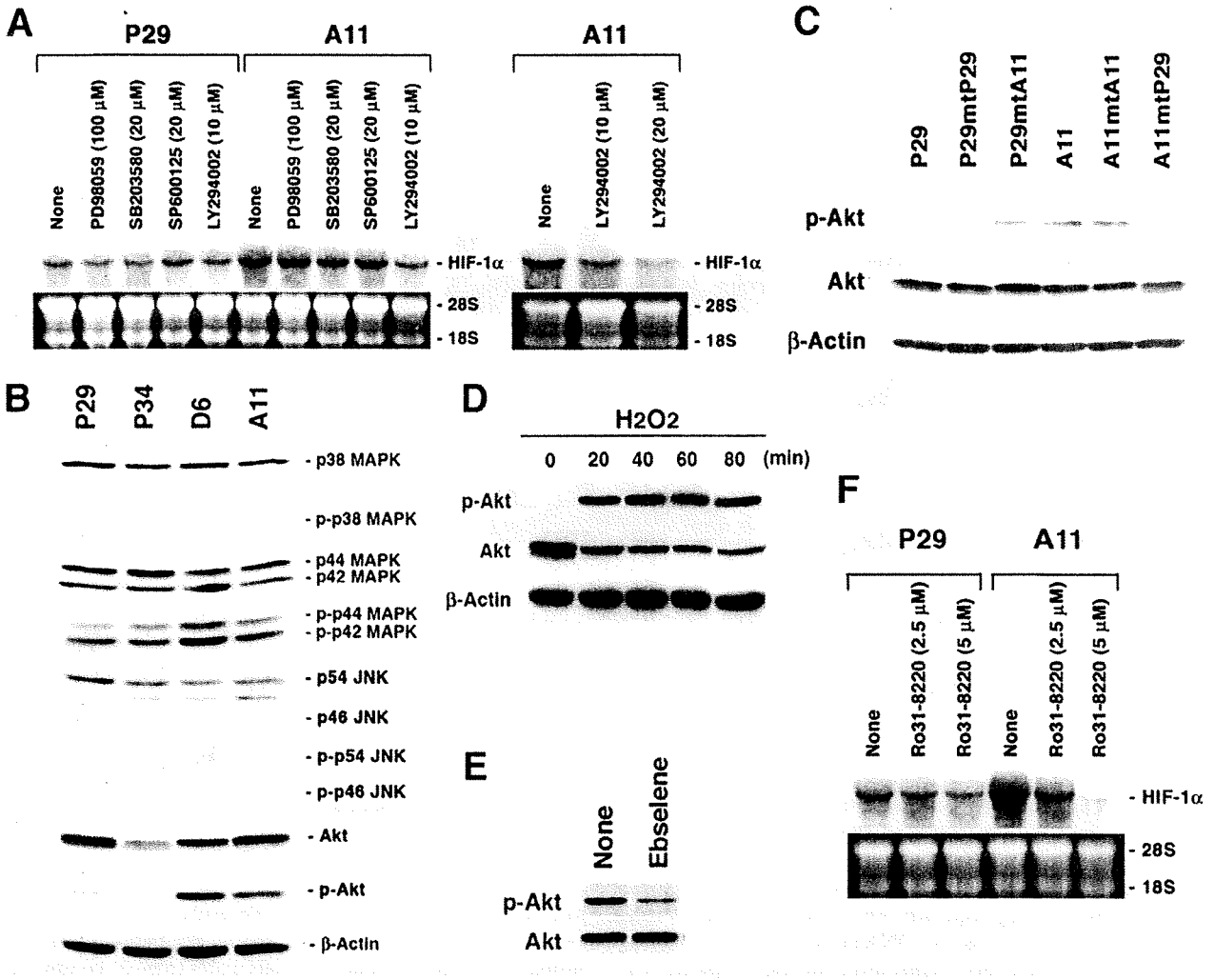

FIGURE 5. **PI3K-Akt and PKC pathways are involved in the ROS-mediated *HIF-1α* mRNA overexpression.** *A*, P29 and A11 cells were treated with dimethyl sulfoxide, PD98059, SB203580, SP600125, and LY294002 at the indicated concentrations for 18 h. Total RNA was extracted and subjected to Northern blot analysis. The blots were hybridized with a ^{32}P-labeled *HIF-1α* cDNA. Ethidium bromide staining of the gel is also shown. *B*, cell lysates prepared from P29, P34, D6, and A11 cells were dissolved by SDS-PAGE. Proteins and phosphorylated proteins and β-actin, which served as a loading control, were detected by immunoblotting. *C*, cell lysates prepared from P29, A11, and the cybrids were subjected to immunoblotting to detect Akt and phosphorylated Akt. β-Actin served as a loading control. *D*, P29 cells were treated with 25 μM H_2O_2 for up to 80 min. Cell lysates were prepared and subjected to immunoblotting as in *C*. *E*, A11 cells were treated with ebselene (20 μM) for 18 h. Cell lysates were prepared and subjected to immunoblotting as in *C*. *F*, P29 and A11 cells were treated with Ro31-8220 at the indicated concentrations for 18 h. Total RNA was analyzed as in *A*.

cin A that inhibits the function of complex III, thereby generating large quantities of superoxide radicals, increased the expression of *HIF-1α* mRNA in both P29 and A11 cells. Fourth, exogenous H_2O_2 enhanced the expression. ROS from NADPH oxidase are also mediators of *HIF-1α* mRNA induction in lipopolysaccharide-stimulated microglial cells and thrombin-stimulated pulmonary artery smooth muscle cells (15, 19). Furthermore, we showed that PI3K-Akt and PKC, but not ERK or JNK, regulate *HIF-1α* mRNA expression. Because both LY29004 and Ro31-8220 suppressed *HIF-1α* mRNA expression more effectively in A11 cells than in P29 cells, PI3K-Akt and PKC may engage in the ROS-mediated expression of *HIF-1α* mRNA. Consistent with these results, either PI3K or PKC or both are shown to regulate *HIF-1α* transcription in lipopolysaccharide-stimulated glial cells, BCR/ABL-expressing Ba/F3 hematopoietic cells, and angiotensin II-treated vascular smooth muscle cells (12, 15, 20). In contrast, ERK and JNK are reported to mediate lipopolysaccharide-stimulated *HIF-1α* mRNA induction in human monocytes/macrophages and hepatoma cells, respectively (21, 22). Further study is required to determine which PKC isoform is responsible for the ROS-mediated expression of *HIF-1α* mRNA using a molecular approach.

The *HIF-1α* gene promoter contains putative binding sites for several transcription factors, including Sp1, AP-1, and NF-κB (23–25). Treatment of A11 cells with mithramycin A resulted in a marked suppression of *HIF-1α* mRNA expression in A11 cells, whereas sulfasarazine and curcumin showed no effect, suggesting the importance of Sp1 for the promoter activity. Luciferase reporter assays also indicated that the Sp1 bind-

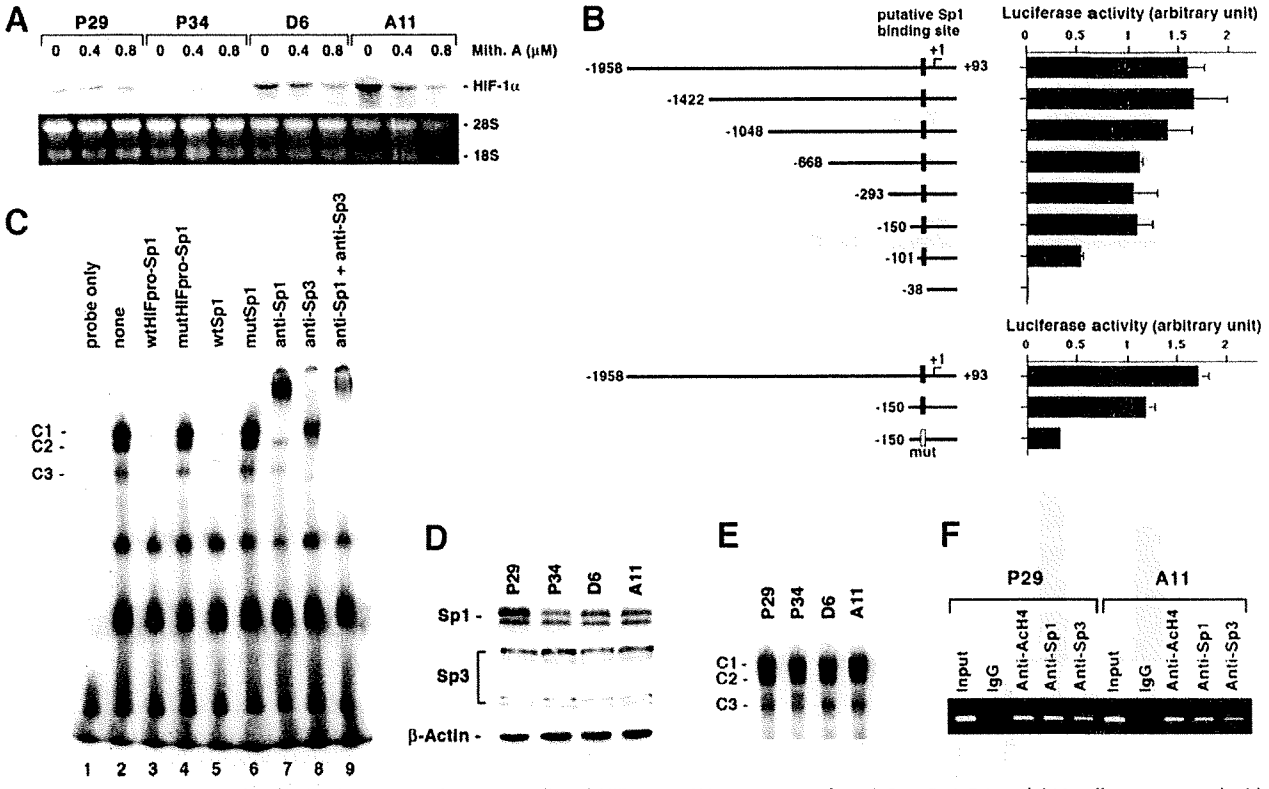

FIGURE 6. **Sp1 is necessary but not sufficient for the ROS-mediated *HIF-1α* mRNA overexpression.** *A*, P29, P34, D6, and A11 cells were treated with mithramycin A at the indicated concentrations for 24 h. Total RNA was extracted and subjected to Northern blot analysis. The blots were hybridized with a ^{32}P-labeled *HIF-1α* cDNA. Ethidium bromide staining of the gel is also shown. *B*, pGL2-basic luciferase reporter plasmids harboring the full-length (−1958/+93) and a series of truncated *HIF-1α* promoters were transfected in A11 cells, and luciferase activity was assayed 45 h after transfection. *Filled* and *open boxes* indicate putative wild-type and mutated Sp1 binding sites, respectively. *C*, nuclear extracts prepared from A11 cells were subjected to EMSAs in which ^{32}P-labeled oligonucleotides (*HIFpro-Sp1*) containing a putative Sp1 binding site was used as a probe. *wtHIFpro-Sp1*, *mutHIFpro-Sp1*, *wtSp1*, and *mutSp1* indicate wild-type HIFpro-Sp1, mutated HIFpro-Sp1, consensus Sp1 and mutated Sp1 oligonucleotides, respectively. *C1–C3* indicate specific Sp-dependent binding complexes. *D*, total cell lysates prepared from P29, P34, D6, and A11 cells were subjected to immunoblotting using anti-Sp1, anti-Sp3 and anti-β-actin antibodies. *E*, nuclear extracts prepared from P29, P34, D6, and A11 cells were subjected to EMSAs as in *C*. *F*, nuclear extracts prepared from P29 and A11 cells were subjected to chromatin immunoprecipitation assays in which anti-acetylated histone H4 (*anti-AcH4*), anti-Sp1, and anti-Sp3 antibodies were used. Normal rabbit IgG served as a control.

ing site is indispensable for the promoter activity. Unexpectedly, however, we could not find any difference in the level of Sp1 binding to and histone acetylation around the binding site between A11 and P29 cells. In contrast, Oh *et al.* (19) reported that lipopolysaccharide induces *HIF-1α* mRNA in an Sp1-dependent pathway. It is necessary to determine whether other regions of the promoter and transcription factors are involved in the overexpression of *HIF-1α* mRNA in A11 cells.

In the present study, we showed that TSA markedly repressed the expression of *HIF-1α* mRNA in A11 cells. Based on this observation, we found a correlation between HDAC activity and *HIF-1α* transcription; that is, HDAC activity was higher in A11 than in P29 cells. It was also higher in H_2O_2-treated P29 cells and antimycin A-treated A11 cells than in the respective control cells. Furthermore, HDAC activity in A11 cells was repressed by ebselene, LY294002, and Ro31-8220. Together, these data indicate that ROS lead to HDAC activation through PI3K and PKC pathways, thereby activating *HIF-1α* transcription. In general, histone acetylation enhances gene expression through the chromatin remodeling caused by histone modification (26). Therefore, it is not clear how HDAC inhibition can lead to the transcriptional repression of the *HIF-1α* gene. However, many genes such as proinflammatory genes, including tumor necrosis factor-α, interleukin-1β, interferon-γ, and inducible nitric-oxide synthase, are reported to be repressed by HDAC inhibitors (27–30). The repression of these proinflammatory genes has been suggested to be a result of inhibition of NF-κB activation and the acetylation of non-histone proteins (30). Because our data indicate little contribution of NF-κB in the ROS-mediated *HIF-1α* mRNA overexpression in A11 cells, acetylation of other non-histone proteins may be important. It should be noted that Noh *et al.* (31) have recently shown that TSA decreases mRNA of extracellular matrix components. They also show that HDAC2 plays an important role in the development of extracellular matrix accumulation and that ROS mediate transforming growth factor-β1-induced activation of HDAC2 (31). HDACs constitute a family of 18 enzymes (32). Therefore, it will be interesting to determine which HDAC is responsible for the ROS-mediated *HIF-1α* transcription in the cells carrying mtDNA with the *ND6* mutation.

In conclusion, our findings show that the ROS-generating *ND6* mutation causes *HIF-1α* transcription via PI3K-Akt/PKC/

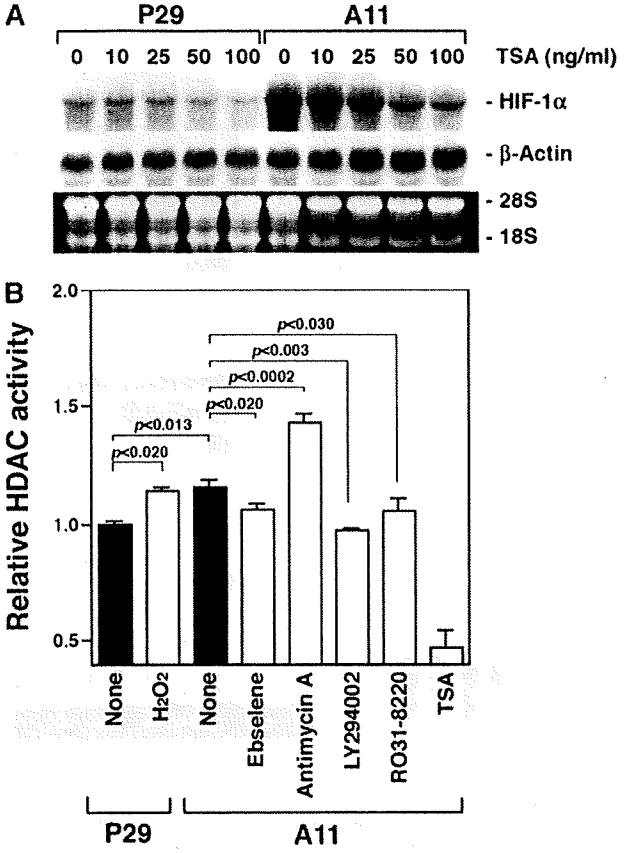

FIGURE 7. **HDAC activity is involved in the ROS-mediated *HIF-1α* transcription.** *A*, P29 and A11 cells were treated with TSA at the indicated concentrations for 18 h. Total RNA was extracted and subjected to Northern blot analysis. The blots were hybridized with a ^{32}P-labeled *HIF-1α* cDNA. Ethidium bromide staining of the gel is also shown. *B*, HDAC activity is shown in untreated P29 and P29 cells treated with 25 μM H_2O_2 for 16 h, and untreated A11 and A11 cells treated with ebselene (20 μM), antimycin A (20 μM), LY294002 (20 μM), Ro31-8220 (5 μM), and TSA (100 ng/ml) for 18 h.

HDAC pathway. Because mtDNA mutations have been implicated to be a factor in cancer etiology and shown to be gradually accumulated in tumor cells, some of them, especially pathogenic somatic mutations, may contribute to malignant progression by causing the up-regulation of HIF-1α protein in tumors.

REFERENCES

1. Brandon, M., Baldi, P., and Wallace, D. C. (2006) *Oncogene* **25,** 4647–4662
2. Park, J. S., Sharma, L. K., Li, H., Xiang, R., Holstein, D., Wu, J., Lechleiter, J., Naylor, S. L., Deng, J. J., Lu, J., and Bai, Y. (2009) *Hum. Mol. Genet.* **18,** 1578–1589
3. Dasgupta, S., Hoque, M. O., Upadhyay, S., and Sidransky, D. (2008) *Cancer Res.* **68,** 700–706
4. Ishikawa, K., Takenaga, K., Akimoto, M., Koshikawa, N., Yamaguchi, A., Imanishi, H., Nakada, K., Honma, Y., and Hayashi, J. (2008) *Science* **320,** 661–664
5. Semenza, G. L. (2009) *Semin. Cancer Biol.* **19,** 12–16
6. Semenza, G. L. (2008) *IUBMB Life* **60,** 591–597
7. Vaupel, P., and Mayer, A. (2007) *Cancer Metastasis Rev.* **26,** 225–239
8. Koshikawa, N., Iyozumi, A., Gassmann, M., and Takenaga, K. (2003) *Oncogene* **22,** 6717–6724
9. Secades, P., Rodrigo, J. P., Hermsen, M., Alvarez, C., Suarez, C., and Chiara, M. D. (2009) *Genes Chromosomes Cancer* **48,** 441–454
10. Saramäki, O. R., Savinainen, K. J., Nupponen, N. N., Bratt, O., and Visakorpi, T. (2001) *Cancer Genet. Cytogenet.* **128,** 31–34
11. Chandel, N. S., McClintock, D. S., Feliciano, C. E., Wood, T. M., Melendez, J. A., Rodriguez, A. M., and Schumacker, P. T. (2000) *J. Biol. Chem.* **275,** 25130–25138
12. Pagé, E. L., Robitaille, G. A., Pouysségur, J., and Richard, D. E. (2002) *J. Biol. Chem.* **277,** 48403–48409
13. Pouysségur, J., and Mechta-Grigoriou, F. (2006) *Biol. Chem.* **387,** 1337–1346
14. Klimova, T., and Chandel, N. S. (2008) *(2008) Cell Death Differ.* **15,** 660–666
15. Bonello, S., Zähringer, C., BelAiba, R. S., Djordjevic, T., Hess, J., Michiels, C., Kietzmann, T., and Görlach, A. (2007) *Arterioscler. Thromb. Vasc. Biol.* **27,** 755–761
16. Koshikawa, N., Maejima, C., Miyazaki, K., Nakagawara, A., and Takenaga, K. (2006) *Oncogene* **25,** 917–928
17. Luo, G., Gu, Y. Z., Jain, S., Chan, W. K., Carr, K. M., Hogenesch, J. B., and Bradfield, C. A. (1997) *Gene Expr.* **6,** 287–299
18. Indo, H. P., Davidson, M., Yen, H. C., Suenaga, S., Tomita, K., Nishii, T., Higuchi, M., Koga, Y., Ozawa, T., and Majima, H. J. (2007) *Mitochondrion* **7,** 106–118
19. Oh, Y. T., Lee, J. Y., Yoon, H., Lee, E. H., Baik, H. H., Kim, S. S., Ha, J., Yoon, K. S., Choe, W., and Kang, I. (2008) *Neurosci. Lett.* **431,** 155–160
20. Mayerhofer, M., Valent, P., Sperr, W. R., Griffin, J. D., and Sillaber, C. (2002) *Blood* **100,** 3767–3775
21. Frede, S., Stockmann, C., Freitag, P., and Fandrey, J. (2006) *Biochem. J.* **396,** 517–527
22. Kim, H. Y., Kim, Y. H., Nam, B. H., Kong, H. J., Kim, H. H., Kim, Y. J., An, W. G., and Cheong, J. (2007) *Exp. Cell Res.* **313,** 1866–1876
23. Iyer, N. V., Leung, S. W., and Semenza, G. L. (1998) *Genomics* **52,** 159–165
24. Minet, E., Ernest, I., Michel, G., Roland, I., Remacle, J., Raes, M., and Michiels, C. (1999) *Biochem. Biophys. Res. Commun.* **261,** 534–540
25. Das, C., and Kundu, T. K. (2005) *IUBMB Life* **57,** 137–149
26. Adcock, I. M. (2007) *Br. J. Pharmacol.* **150,** 829–831
27. Joseph, J., Mudduluru, G., Antony, S., Vashistha, S., Ajitkumar, P., and Somasundaram, K. (2004) *Oncogene* **23,** 6304–6315
28. Leoni, F., Zaliani, A., Bertolini, G., Porro, G., Pagani, P., Pozzi, P., Donà, G., Fossati, G., Sozzani, S., Azam, T., Bufler, P., Fantuzzi, G., Goncharov, I., Kim, S. H., Pomerantz, B. J., Reznikov, L. L., Siegmund, B., Dinarello, C. A., and Mascagni, P. (2002) *Proc. Natl. Acad. Sci. U.S.A.* **99,** 2995–3000
29. Yu, Z., Zhang, W., and Kone, B. C. (2002) *J. Am. Soc. Nephrol.* **13,** 2009–2017
30. Quivy, V., and Van Lint, C. (2004) *Biochem. Pharmacol.* **68,** 1221–1229
31. Noh, H., Oh, E. Y., Seo, J. Y., Yu, M. R., Kim, Y. O., Ha, H., and Lee, H. B. (2009) *Am. J. Physiol. Renal. Physiol.* **297,** 729–739
32. Witt, O., Deubzer, H. E., Milde, T., and Oehme, I. (2009) *Cancer Lett.* **277,** 8–21

THE JOURNAL OF BIOLOGICAL CHEMISTRY VOL. 284, NO. 51, pp. 35433–35440, December 18, 2009

TATA-binding Protein (TBP)-like Protein Is Engaged in Etoposide-induced Apoptosis through Transcriptional Activation of Human *TAp63* Gene*[S]

Received for publication, July 30, 2009, and in revised form, October 20, 2009 Published, JBC Papers in Press, October 26, 2009, DOI 10.1074/jbc.M109.050047

Yusuke Suenaga[‡§], Toshinori Ozaki[§], Yuji Tanaka[‡], Youquan Bu[§], Takehiko Kamijo[§], Takeshi Tokuhisa[¶], Akira Nakagawara[§1], and Taka-aki Tamura[‡2]

From the [‡]Graduate School of Science, Chiba University, 1-33 Yayoicho, Inage-ku, Chiba 263-8522, the [§]Division of Biochemistry, Chiba Cancer Center Research Institute, 666-2 Nitona, Chuoh-ku, Chiba 260-8717, and the [¶]Department of Developmental Genetics, Graduate School of Medicine, Chiba University, Chiba 260-8670, Japan

Accumulating evidence indicates that TBP (TATA-binding protein)-like protein (TLP) contributes to the regulation of stress-mediated cell cycle checkpoint and apoptotic pathways, although its physiological target genes have remained elusive. In the present study, we have demonstrated that human *TAp63* is one of the direct transcriptional target genes of TLP. Enforced expression of TLP results in the transcriptional induction of the endogenous *TAp63*, but not of the other *p53* family members such as *TAp73* and *p53*. Consistent with these results, small interference RNA-mediated knockdown led to a significant down-regulation of the endogenous *TAp63*. Luciferase reporter assay and chromatin immunoprecipitation analysis revealed that the genomic region located at positions −487 to −29, where +1 represents the transcriptional initiation site of *TAp63*, is required for TLP-dependent transcriptional activation of *TAp63* and also TLP is efficiently recruited onto this region. Additionally, cells treated with anti-cancer drug etoposide underwent apoptosis in association with the transcriptional enhancement of *TAp63* in a p53-independent manner, and the knockdown of the endogenous TLP reduced etoposide-induced apoptosis through repression of *TAp63* expression. Taken together, our present study identifies a TLP-TAp63 pathway that is further implicated in stress-induced apoptosis.

Transcriptional regulation involves the functional integration of diverse factors and is a critical regulatory step for cellular events that include growth, differentiation, and death. These cellular activities often occur simultaneously due to the action of regulatory factors with broad targets. A representative example of such a factor is the tumor suppressor p53 and its family members, including p63 and p73, which contribute to tumor suppression, cell cycle checkpoint, DNA repair, and apoptosis (1). p63 acts as a pro-apoptotic transcription factor (2, 3) and, like p53 and p73, is expressed as multiple isoforms (4). They include the *trans*-activating (TA)[3] isoform of p63, termed TAp63, and an NH_2-terminal activation domain-deficient isoform, ΔNp63, that acts as a dominant negative factor over p53, TAp63, and TAp73 (2). p63 has been clearly implicated in a variety of developmental processes (5), whereas its anticipated role as a tumor suppressor is unclear, mainly because of its low frequency of the somatic mutations in human tumors (6, 7). However, a study focused on long term effects of *p63* mutations in mice showed that mice bearing mutations in both *p63* and *p53* develop a more aggressive tumor, indicating the presence of a tumor suppressive activity of p63 (8). This is consistent with earlier studies indicating that p63 is required for p53-dependent apoptotic response (9) and that, in response to certain DNA damage insults, p63 activates an overlapping set of p53-target genes implicated in cell cycle arrest and apoptosis (10). Although extensive studies of p63 in human tumors have suggested that deregulated expression of TAp63 and ΔNp63 contributes to tumor development and progression (4), the precise molecular mechanisms behind the transcriptional regulation of *TAp63* remain to be unclear.

TATA-binding protein (TBP) is a general transcription factor that plays a central role in the regulation of pre-initiation complex formation by eukaryotic RNA polymerases (11, 12). Eukaryotic cells also contain multiple TBP paralogs implicated in transcriptional regulation during cell growth, differentiation, and development (11, 12). TBP-like protein (TLP) (13), also known as TBP-related factor 2 (14, 15), TLF (16), or TRP (17), is one of the TBP paralogs common to Metazoa and has been implicated by genetic studies in various developmental processes, including spermiogenesis in mice (11, 12). Although TLP fails to bind to TATA box (11, 12), it stimulates transcription from several TATA-less promoters (18). Mammalian TLP, unlike TBP, does not associate with TAFs to form a transcrip-

* This work was supported by a Grant-in-Aid from the Ministry of Health, Labor and Welfare for Third Term Comprehensive Control Research for Cancer (to A. N.), a Grant-in-Aid for Scientific Research on Priority Areas from the Ministry of Education, Culture, Sports, Science and Technology, Japan (to T. T. and A. N.), a Grant-in-Aid for Scientific Research from Japan Society for the Promotion of Science (to A. N.), and grants from Uehara Memorial Foundation and Futaba Corporation (to T. T. and A. N.).

[S] The on-line version of this article (available at http://www.jbc.org) contains supplemental Figs. S1–S3.

[1] To whom correspondence may be addressed: Division of Biochemistry, Chiba Cancer Center Research Institute, 666-2 Nitona, Chuou-ku, Chiba 260-8717, Japan. Tel.: 81-43-264-5431; Fax: 81-43-265-4459; E-mail: akiranak@chiba-cc.jp.

[2] To whom correspondence may be addressed. Tel.: 81-43-290-2823; Fax: 81-43-290-2824; E-mail: ttamura@faculty.chiba-u.jp.

[3] The abbreviations used are: TA, *trans*-activating isoform; ChIP, chromatin immunoprecipitation; FACS, fluorescence-activated cell sorter; NF1, neurofibromatosis type 1; siRNA, small interfering RNA; TBP, TATA-binding protein; TLP, TBP-like protein; TUNEL, terminal deoxynucleotidyl transferase-mediated dUTP nick end labeling; RT, reverse transcription.

tion factor IID-type complex but, instead, associates with TFIIA in cells (14, 19). It was reported earlier (20) that mammalian TLP activates transcription from the TATA-less neurofibromatosis type 1 (*NF1*) promoter through site-specific binding, but represses the TATA-containing c-*fos* promoter, thus leading to the prediction of an anti-oncogenic ability of TLP as well as the potential for direct binding to other target genes. Shimada *et al.* (21) reported that chicken TLP represses the G_2/M transition and, through its nuclear translocation, mediates apoptosis induction in a p53-independent manner. Hence, TLP is proposed to have both checkpoint and anti-oncogenic functions, although its physiological role and also the precise molecular mechanisms behind TLP-mediated apoptosis as well as cell cycle checkpoint remain to be elusive.

Here, we have analyzed mammalian TLP function in relation to TAp63 expression and show that TLP enhances the promoter activity of *TAp63* and thus leads to apoptosis. Further observations suggest that this novel TLP-TAp63 pathway increases the sensitivity to anti-cancer drug etoposide.

EXPERIMENTAL PROCEDURES

Cell Culture and Transfection—Chicken DT40 cells were grown in RPMI 1640 medium (Invitrogen) as previously described (21). DT40-TLP$^{-/-}$ cells derived from parental DT40 cells lack *TLP* (21). Human cervical carcinoma-derived HeLa and human hepatocellular carcinoma-derived HepG2 cells were cultured in Dulbecco's modified Eagle's medium (Invitrogen) supplemented with 10% heat-inactivated fetal bovine serum (Invitrogen), penicillin (100 IU/ml), and streptomycin (100 μg/ml). Human hepatocellular carcinoma-derived Hep3B cells were grown in RPMI 1640 medium supplemented with 10% heat-inactivated fetal bovine serum and antibiotics. HepG2 and HeLa cells carry wild-type *p53*. Hep3B and DT40 cells lack *p53*. Where indicated, cells were exposed to etoposide (at a final concentration of 50 μM). For transfection, DT40 cells were transiently transfected with the indicated expression plasmids by electroporation. HeLa cells were transiently transfected with the indicated combinations of the expression plasmids using Lipofectamine 2000 transfection reagent (Invitrogen) according to the manufacturer's instructions.

RT-PCR—Total RNA was prepared from the indicated cells using RNeasy Mini Kit (Qiagen, Valencia, CA) according to the manufacturer's recommendations. For the RT-PCR, first strand cDNA was generated using SuperScript II reverse transcriptase (Invitrogen) and random primers. The resultant cDNA was subjected to the PCR-based amplification. The oligonucleotide primers used in this study were as follows: human *TLP*, 5′-CCTCTTCCCACGGATGTGAT-3′ (sense) and 5′-GAGTCCAATGTGCAGCAGT-3′ (reverse); mouse *TLP*, 5′-GCCATTTGAACTTAAGGA-3′ (forward) and 5′-TGTAAATTCTGGCAA-3′ (reverse); human *TAp63*, 5′-GTCCCAGAGCACACAGACAA-3′ (forward) and 5′-GAGGAGCCGTTCTGAATCTG-3′ (reverse); chicken *TAp63*, 5′-GAAACAGCCATGCCCAGTAT-3′ (forward) and 5′-CAAATGCGAGCTTCAAAACA-3′ (reverse); human *TAp73*, 5′-CGGGACGGACGCCGATG-3′ (forward) and 5′-GAAGGTCGAAGTAGGTGCTGTCTGG-3′ (reverse); human *p53*, 5′-ATTTGATGCTGTCCCCGGACGATATTGAAC-3′ (forward) and 5′-ACCCTTTTTGGACTTCCGGACGATATTGAAC-3′ (reverse); human p21^{waf1}, 5′-GACACCACTGGAGGGTGACT-3′ (forward) and 5′-CCCTAGGCTGTGCTCACTTC-3′ (reverse); human 14-3-3σ, 5′-AGAGCGAAACCTGCTCTCAG-3′ (forward) and 5′-CTCCTTGATGAGGTGGCTGT-3′ (reverse); human *Lamin A/C*, 5′-CCGAGTCTGAAGAGGTGGTC-3′ (forward) and 5′-AGGTCACCCTCCTTCTTGGT-3′ (reverse); human *BAX*, 5′-TCTGACGCAACTTCAACAC-3′ (forward) and 5′-GAGGAGTCTCACCCAACCAC-3′ (reverse); human *PUMA*, 5′-GCCCAGACTGTGAATCCTGT-3′ (forward) and 5′-TCCTCCCTCTTCCGAGATTT-3′ (reverse); human *NOXA*, 5′-GCAAGAATGGAAGACCCTTG-3′ (forward) and 5′-GTGCTGAGTTGGCACTGAAA-3′ (reverse); human *GAPDH*, 5′-ACCTGACCTGCCGTCTAGAA-3′ (forward) and 5′-TCCACCACCCTGTTGCTGTA-3′ (reverse). The expression of β-*actin* or *GAPDH* was measured as an internal control. The PCR products were subjected to 1% agarose gel electrophoresis and visualized by ethidium bromide staining.

Real-time Quantitative RT-PCR—Total RNA was extracted from clinical samples using TRIzol reagent (Invitrogen) according to the manufacturer's instructions, and reverse transcription was performed with SuperScript II reverse transcriptase (Invitrogen). Real-time quantitative PCR (TaqMan PCR) using an ABI Prism 7700 sequence detection system (Perkin-Elmer Applied Biosystems, Foster City, CA) was carried out according to the manufacturer's protocol. All the reactions were performed in triplicate. The data were averaged from the values obtained in each reaction. The mRNA levels of each of the genes were standardized by β-*actin*.

siRNA—Hep3B cells transiently transfected with siRNA targeting TLP (TLP siRNA-1, 5′-UAACAGGGCCCAAUGUAAA-3′; TLP siRNA-2, 5′-GGAAGGAGCAAAUGUAAUU-3′), siRNA against TAp63 (TAp63 siRNA-1, 5′-CAGCUAUAUGUUCAGUUC-3′; TAp63 siRNA-2, 5′-GAUUGAGAUUAGCAUGGAC-3′) (Invitrogen) or with siRNA against Lamin A/C (Dharmacon, Chicago, IL) by using Lipofectamine RNAiMAX transfection reagent (Invitrogen) according to the manufacturer's instructions. Forty-eight hours after transfection, total RNA was prepared and processed for RT-PCR.

Immunoblotting—Cells were washed in ice-cold phosphate-buffered saline and lysed in an SDS-sample buffer. After brief sonication, whole cell lysates were boiled for 5 min, resolved by 12% SDS-PAGE, and electrotransferred onto Immobilon-P membranes (Millipore, Bedford, MA). The membranes were blocked with Tris-buffered saline containing 0.1% Tween 20 and 5% nonfat dry milk and then incubated with monoclonal anti-p21^{waf1} (Ab-1, Oncogene Research Products, Cambridge, MA), monoclonal anti-FLAG (M2, Sigma), monoclonal anti-Lamin B (Ab-1, Calbiochem), monoclonal anti-tubulin-α (Ab-2, Neomarkers, Fremont, CA), polyclonal anti-TAp63 (22), polyclonal anti-TLP (23), or with polyclonal anti-actin (20-33, Sigma) antibody for 1 h at room temperature followed by an incubation with the appropriate horseradish peroxidase-conjugated secondary antibodies (Jackson ImmunoResearch Laboratories, West Grove, PA) for 1 h at room temperature. The

chemiluminescence reaction was performed using ECL reagent (Amersham Biosciences, Piscataway, NJ).

Construction of Luciferase Reporter Plasmids—A luciferase reporter plasmid containing *TAp63* promoter region encompassing from −2340 to +26, where +1 represents the transcriptional initiation site, was amplified by PCR-based strategy using genomic DNA prepared from human placenta as a template. Oligonucleotide primers used were as follows: F1, 5′-TTGGTAGAGCTCGAGGATAGCTTGAGTCCAGCAG-3′ (forward) and R1, 5′-AGATATCCCTTTCACATCCC-3′ (reverse); F2, 5′-GTGCATGTGTTTGAGGTAGG-3′ (forward) and R2, 5′-CTTAGAGCTAGCCCTTCAACTGTCTTTGATATCAACG-3′ (reverse). Underlined sequences indicate the positions of SacI restriction site in the forward primer F1 and NheI restriction site in the reverse primer R2. PCR products were gel-purified and subcloned into pGEM-T Easy plasmid (Promega, Southampton, UK) according to the manufacturer's protocol. The resultant plasmid DNA was digested with SacI plus HindIII or with HindIII plus NheI and then subcloned into SacI/NheI restriction sites of pGL3-basic plasmid (Promega) to give pGL3-TAp63(−2340). A series of the 5′ deletion mutants of pGL3-TAp63(−2340) were generated by using an Erase-A-Base system (Promega) according to the manufacturer's instructions.

Luciferase Reporter Assay—HeLa cells were transiently co-transfected with the constant amount of the indicated pGL3-TAp63 luciferase reporter constructs (100 ng), pRL-TK *Renilla* luciferase reporter plasmid (10 ng) together with or without 100 ng of the expression plasmid for FLAG-TLP. The total amount of the plasmid DNA per each transfection was kept constant (510 ng) with the empty plasmid (pCIneo). Forty-eight hours after transfection, cells were harvested and lysed, and both firefly and *Renilla* luciferase activities were measured by using a Dual-Luciferase reporter assay system (Promega). The firefly luminescence signal was normalized based on the *Renilla* luminescence signal.

ChIP Assay—Chromatin immunoprecipitation (ChIP) assay was performed according to the protocol provided by Upstate Biotechnology (Charlottesville, VA). In brief, HeLa cells were transiently transfected with the expression plasmid for FLAG-TLP. Forty-eight hours after transfection, cells were cross-linked with 1% formaldehyde in medium at 37 °C for 15 min. Cells were then washed in ice-cold phosphate-buffered saline and resuspended in 200 μl of SDS lysis buffer containing protease inhibitor mixture. The suspension was sonicated on ice and pre-cleared with protein A-agarose beads blocked with sonicated salmon sperm DNA (Upstate Biotechnology) for 30 min at 4 °C. The beads were removed, and the chromatin solution was immunoprecipitated with polyclonal anti-FLAG (Sigma) antibody at 4 °C, followed by incubation with protein A-agarose beads for an additional 1 h at 4 °C. The immune complexes were eluted with 100 μl of elution buffer (1% SDS and 0.1 M $NaHCO_3$), and formaldehyde cross-links were reversed by heating at 65 °C for 6 h. Proteinase K was added to the reaction mixtures and incubated at 45 °C for 1 h. DNA of the immunoprecipitates and control input DNA were purified and then analyzed by standard PCR using human *TAp63* promoter-specific primers.

Subcellular Fractionation—To prepare nuclear and cytoplasmic extracts, cells were lysed in 10 mM Tris-HCl, pH 7.5, 1 mM EDTA, 0.5% Nonidet P-40, 1 mM phenylmethylsulfonyl fluoride, and a protease inhibitor mix (Sigma) and centrifuged at 5000 rpm for 10 min to collect soluble fractions, which were referred to as cytosolic extracts. Insoluble materials were washed in the lysis buffer and further dissolved in SDS-sample buffer to collect the nuclear extracts. The nuclear and cytoplasmic fractions were subjected to the immunoblot analysis using monoclonal anti-Lamin B (Ab-1, Oncogene Research Products) or monoclonal anti-tubulin-α (Ab-2, Neomarkers) antibody.

TUNEL Staining—Hep3B cells were grown on coverslips and transiently transfected with the indicated siRNAs. Forty-eight hours after transfection, cells were fixed in 4% paraformaldehyde and apoptotic cells were detected by using an *in situ* cell detection Kit (Roche Molecular Biochemicals, Mannheim, Germany) according to the manufacturer's protocol. The coverslips were mounted with 4′,6-diamidino-2-phenylindole-containing mounting medium (Vector Laboratories, Burlingame, CA) and observed under a Fluoview laser scanning confocal microscope (Olympus, Tokyo, Japan).

FACS Analysis—Transfected HepG2 cells were exposed to 50 μM of etoposide. Forty-eight hours after the treatment, floating and attached cells were collected, washed in ice-cold phosphate-buffered saline, and fixed in 70% ethanol at −20 °C. Following incubation with phosphate-buffered saline containing 40 μg/ml of propidium iodide and 200 μg/ml of RNase A for 1 h at room temperature in the dark, stained nuclei were analyzed by a FACScan machine (BD Biosciences, Mountain View, CA).

Statistical Analysis—The data obtained from real-time PCR were expressed as means ± S.E. of the mean.

RESULTS

TLP Has an Ability to Induce the Expression of TAp63—We have previously described that TLP induces both cell cycle arrest and apoptosis in chicken DT40 cells in a p53-independent manner (21). These results imply that the other p53 family members such as p73 or p63 could be closely involved in these cellular processes, because p53 family members play a dominant role in the regulation of cell fate determination. To examine the possible contribution of TLP to *p53*, *TAp73*, and *TAp63* gene expression, human cervical carcinoma-derived HeLa cells were transiently transfected with FLAG-TLP expression plasmid. Intriguingly, enforced expression of FLAG-TLP resulted in a significant up-regulation of *TAp63* but not of *p53* and *TAp73* (Fig. 1, *A* and *B*). Consistent with these results, siRNA-mediated knockdown of the endogenous *TLP* led to a remarkable down-regulation of the endogenous *TAp63* as well as its direct transcriptional target genes such as $p21^{waf1}$ and *NOXA* (Fig. 1*C*). $p21^{waf1}$ and NOXA are involved in the induction of cell cycle arrest and apoptosis, respectively (24). Additionally, knocking down of the endogenous *TAp63* had an undetectable effect on the expression level of the endogenous *TLP*, whereas the expression levels of the endogenous $p21^{waf1}$ and *NOXA* dramatically decreased. In support with these results, *TLP*-deficient chicken DT40 cells expressed *p63* at an extremely lower level as compared with wild-type DT40 cells, and ectopic